Combined Exergy Analysis and Energy Integration for the Optimization of Nitrogen Fertilizer Plants

Daniel Flórez-Orrego[a], Shivom Sharma[b], Silvio de Oliveira Junior[c], François Maréchal[d]

[a,c] Polytechnic School, University of Sao Paulo, Brazil, [a]daflorezo@usp.br CA, [c]soj@usp.br,*
[a,b,d] École Polytechnique Fédérale de Lausanne, Switzerland, [b]shivom.sharma@epfl.ch, [d]francois.marechal@epfl.ch

Modern ammonia production plants are equipped with efficient energy integration networks able to recover an important fraction of the enthalpy of reaction released by the exothermic chemical systems. However, to fully supply the exergy demands of the highly endothermic reforming reaction, the syngas purification and compression systems, an additional energy consumption, typically provided by means of costly non-renewable resources, is still required. Consequently, an optimal energy integration of the reactive components to the remaining systems of the plant might allow not only reducing the amount of fuel consumed, but also minimizing the process irreversibility by pursuing enhanced heat recovery and power generation. Furthermore, the valorization of the byproducts (e.g. CO_2) may also increase the overall efficiency of the process, whereas the reduction of wastes ensures a minimum degradation of valuable feedstock. On the other hand, the choice of a carbon capture unit based on either physical or chemical absorption drastically affects the way in which the waste heat recovery (e.g. combustion air preheating) must be performed, and whether one or more energy technologies should or not be integrated (e.g. heat pump). Furthermore, the selection among various energy resources, such as the import of electricity over the autonomous combined heat and power production (CHP), strongly depends on the ratio between the prices of electricity and fuels consumed, as well as on the extent of the energy integration. Thus, evidently, a simple trial and error approach falls short in efficiently determining the most suitable energy technologies and the operating conditions that enable the chemical plant to operate under minimum cost. Accordingly, in this work, a systematic methodology is used to identify the most suitable utility systems (cooling, refrigeration, and cogeneration) that satisfy the minimum energy requirement (MER) with the lowest energy consumption and operating cost. In addition, the exergy analysis is used to identifying potential improvements that may remain hidden to conventional energy integration analyses, regarding the minimization of the avoidable exergy losses and the integration of reactive, CHP and syngas purification systems. By applying this methodology, the best operating condition and size of such systems are identified, as well as the opportunities for producing surplus electricity in complex ammonia production plants, typically associated to urea and nitric acid production facilities in SNF complexes.

Keywords: Pinch analysis, Minimum energy requirement, Exergy destruction, Fertilizers.

1. Introduction

Despite the increasing domestic production [1, 2], more than 60% of the nitrogen fertilizers consumed in Brazil must still be imported [3]. This leaves the country vulnerable to variations of prices in the international markets, including oil and natural gas prices, shipping costs and logistical problems at ports [4]. In fact, fertilizers industry is the segment that has contributed the most (25%) towards the total deficit in the Brazilian chemical sector [5]. The main technological and economic lags are owed to the use of old existent plants relying on less efficient practices and conversion technologies. Thus, aiming to reduce the foreign dependence of the Brazilian fertilizers sector to only 13% by 2020 [6], the government has contemplated further investments in the construction of new (or revamping old) plants [3, 5-7]. On the other hand, the manufacture of SNF is an energy intensive industry that fundamentally

depends on the consumption of large amounts of non-renewable resources, contributing further to the environmental strain already associated to extensive farming. Consequently, SNF plants have deserved an increased legal surveillance in the last years, having to comply with more stringent controls of atmospheric emissions and waste production. Thus, in order to fulfill the new regulations, SNF research and technology has undergone radical developments in terms of both design and equipment, most of them focused on the reduction of the power and feedstock demands, the improvement of the waste heat recovery network, and the design of better and more active catalysts.

Worrell and Blok [8] calculated the energy savings in the manufacturing of several nitrogen fertilizers, including ammonia, by considering the theoretical minimum energy consumption using the steam methane reforming route. The authors suggested that profitable energy savings would be only obtained by means of technical breakthroughs, such as higher ammonia conversions at lower pressures and more efficient heat exchange systems. Later, Kirova-Yordanova [9] discussed whether a standalone combined heat and power production (CHP) system would be more efficient than thermally integrating the chemical plant to a waste heat recovery system for supplying the required plant utilities. The author concludes that the decision-making is strongly dependent on the efficiency of the chemical plant equipment and the CHP system. However, an enhanced integration of the steam network with the chemical plant might actually lead to a 10% lower energy consumption compared to a standalone CHP unit [10]. Also according to Kirova-Yordanova [11], the exergy consumption in the ammonia synthesis loop is highly dependent on the designed setup, and at least 61% of the destroyed exergy comes from the ammonia converter. As a result, the best way to reduce energy consumption and, thus, to improve the overall exergy efficiency of the ammonia unit, is by means of the maximum recovery of the enthalpy of the reaction at a higher level of temperature for high pressure steam generation.

Panjeshahi et al. [12] studied the retrofitting opportunities of an existing ammonia plant based on suitable modifications of the existing heat exchanger network, especially in the reformer convection train, which is separately considered as a hot threshold problem. The Carnot grand composite curve derived from a combined *pinch* and exergy analysis was used to determine the extent of the integration of the refrigeration cycle already in use, a well as to suggest the most appropriate temperature levels that reduce the system irreversibility and shaft power consumption. Leites et al. [13] determined the causes of the thermodynamic irreversibility in chemical reactors and other industrial chemical processes in the ammonia plants based on the counteraction principle. It is shown that conflicting objectives may arise from the minimization of the process irreversibility while simultaneously aiming to increase the driving forces, with special attention to reactive separation and exothermic reactors. Sorin and Paris [14] used the exergy load distribution method in a typical hydrogen production unit using steam methane reforming. It is found that a small reduction (15°C) in the high temperature shift reactor produces a 2% increase in hydrogen yield at the expense of 1.4% of the exportable steam, without requiring any equipment modifications. In spite of this comprehensive research on energy integration and optimization achieved so far, the minimum theoretical consumption in ammonia plants is still much lower (18-21GJ/t_{NH3}) than the best figures reported (28-31 GJ/t_{NH3}) [15], which vary widely with local conditions and project-specific requirements [10, 16]. Thus, according to the

European Roadmap of Process Intensification (PI - PETCHEM), the potential benefits in the ammonia production sector are significant. In the short to mid-term (10-20 years), an increase of 5 percent in the overall energy efficiency is expected, whereas 20 percent higher energy efficiency is envisaged in the long term (30-40 years) [17]. Other studies [18] are less optimistic and estimate more moderate improvement rates than those experienced over the 1991-2003 period. For instance, the improvement in the fuel consumption is predicted to be 35% lower than during the previous decade. Despite those promising figures, it must be born in mind that any additional room for efficiency increase or reduced environmental impact might not come about but through breakthrough approaches [19, 20], including radical diversification of the energy resources in the fertilizers sector [21-23]. Moreover, non-conventional approaches for the enhanced integration have not been fully industrially exploited so far mainly due to technical or economic aspects. These attempts include more active catalyst operating at lower temperatures [24], monolith reactors [25], low-grade temperature heat valorization, thermally coupled [26] or in situ adsorption reactors [27] and reactor effluent expansion [28, 29]. Although it could take too long for those systems to be commercially accomplished, only by studying novel configurations, a deeper insight into the thermodynamic limitations that the reduction of the energy consumption in ammonia plants copes with could be seized. However, new components and facilities also require high initial capital investments, whereas retrofitting the old ones poses several challenges in terms of off-design and increased operational flows. In fact, retrofitting existing plants is a troublesome enterprise as these facilities already consist of complexly integrated setups coupled via mass and energy flows, and recycling streams. This circumstance renders the overall system analysis not only large in magnitude, but also the interdependencies lead to a complex non-linear problem.

Accordingly, in order to compare the benefits of revamping or substituting the outdated technologies, a systematic framework is required. Papoulias and Grossman [30-33] presented a strategy based on the mixed-integer linear programming (MILP) for the optimal synthesis of a chemical plant explicitly accounting for the interactions among the chemical plant and the utility systems. Later, Maréchal and Kalitvenzeff [34] and Maréchal et al. [35] also proposed a mathematical programming strategy to determine the most suitable energy sources and utility systems for a chemical plant employing a MILP approach, this latter used in this paper. Thus, an extended assessment encompassing the feedstock supply chain and conversion stages in an integrated syngas and ammonia production plant is performed. The utility systems and their operating loads that minimize the operating costs of a steam methane reforming (SMR) based ammonia production plant are determined. In addition, the exergy analysis is used to identify potential improvements that may remain hidden to the conventional energy integration analysis, especially as it comes to the integration of reactive systems and combined heat and power production (CHP).

2. Plantwide process description

Figure 1 shows the simplified layout of an integrated syngas and ammonia production plant based on the steam reforming of natural gas. The chemical plant is composed of the syngas production unit (feedstock saturator, prereformer, primary and secondary reformers and water gas shift reactors), the syngas purification process (CO_2 removal by either a physical or a chemical absorption system and a

methanator), and the ammonia synthesis (multiple reactor beds with intercooling) and separation processes (condensation and refrigeration systems). Since these elements are strongly interrelated to each other, it is expected the operating conditions of a set of components to be simultaneously affected by the performance of the remaining sections of the plant concept, especially the heat and power balance of the whole plant.

2.1. Chemical process units

According to Fig. 1, the natural gas feedstock fed to the primary reformer is mixed to the process steam in typical steam to carbon ratios (S/C) between 2.5-4.0, depending on the feedstock used, the purge gas recovery, the reformer capacity, the shift operating conditions and the plant steam balance [36]. Steam can be produced either by means of standalone auxiliary boilers or through heat recovery steam generators that recover the waste heat produced along the chemical plant. A special device called saturator simultaneously saturates the natural gas while injects and vaporizes the process water. The saturated syngas is then sent to an adiabatic reactor located upstream of the primary reformer called prereformer [15]. Therein, the reactions (R.1-R.2) are partially achieved at lower temperatures (< 600°C) than in the primary reformer, thus converting the heavier hydrocarbons and alleviating the firing at the reformer's furnace [13]. Since the prereformer is slightly endothermic, the mixture must be reheated previously to its conversion in the primary reformer. Some authors reported a reduction of up to 10% of the natural gas consumption when a prereformer is used [13, 37, 38]. The primary reforming is by far the most exergy-intensive processes, requiring a thermal duty above 50 MW [39] for a typical 1000 t_{NH3}/day plant. This duty is generally supplied by a radiant combustion furnace capable of sustaining the highly endothermic reactions occurring in the catalytic tubes, whereas the residual exergy of the flue gas can be utilized for raising and superheating steam, as well as to preheat other process streams [40]. High temperatures and moderate pressures, as well as a fairly larger steam to carbon ratios (SC > 3) favor the equilibrium of the methane reforming reaction (R.1), reduce the methane slip and avoid the carbon deposits on the catalyst.

$$CH_4 + H_2O \rightarrow CO + 3H_2 \qquad \Delta H^o_{298} = 206\ kJ\ mol^{-1} \qquad \text{R.1}$$

$$CO + H_2O \rightarrow CO_2 + H_2 \qquad \Delta H^o_{298} = -41\ kJ\ mol^{-1} \qquad \text{R.2}$$

A lined secondary reformer is used to introduce the nitrogen into the process stream (N_2/H_2 = 3:1) by partially burning the reformed mixture from the primary reformer with air, setting both the required stoichiometry and heat balance. Process air compression accounts for about one third of the total power consumed in the plant [39]. Next, the secondary reformer effluent is cooled down to a feed temperature suitable for the high and low temperature water gas shift reactors, where an additional amount of hydrogen is produced at the expense of the CO and water content in the syngas (R.2). The CO_2 produced is commonly removed by scrubbing the syngas with chemical absorption agents like di-ethanol (DEA) and methyl di-ethanol (MDEA) amines or physical absorption agents, such as dimethyl ethers of polyethylene glycol (DEPG).

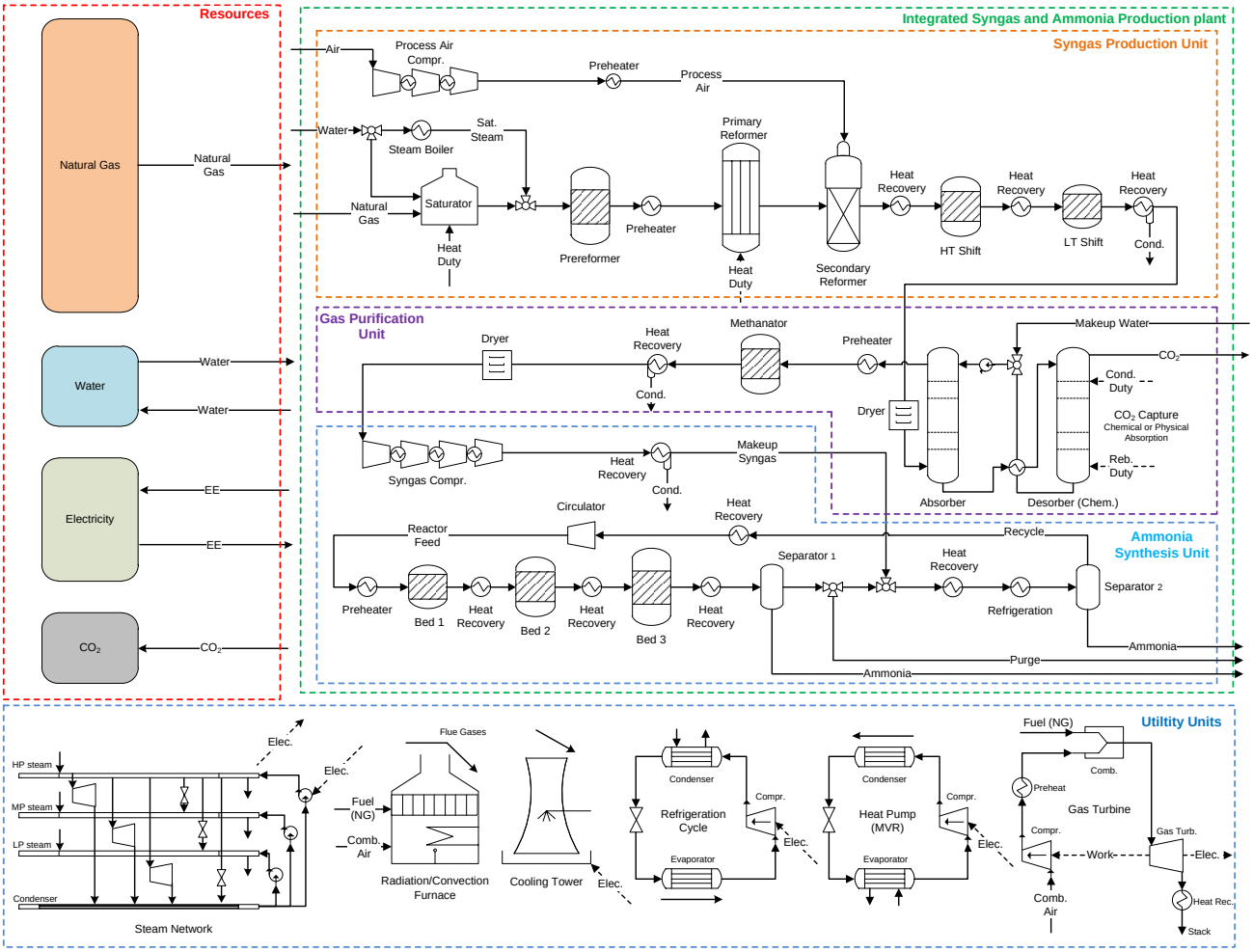

Fig. 1. Superstructure of the chemical processes, utility units and resources network of an integrated syngas and ammonia production plant.

Figure 2 compares the two chemical and physical absorption units analyzed in this work. In the chemical absorption systems, the solvent is regenerated by stripping out the CO_2 gas using either waste heat or low pressure steam. Despite its lower rate of CO_2 absorption and, consequently, higher solvent recirculation rates, MDEA has lower desorber energy requirements and improved chemical stability, and allows for higher acid gas loadings and solution strengths than DEA. Thus, the addition of primary (MEA) or secondary amines (DEA) helps increasing significantly the rate of absorption without compromising the desirable MDEA properties [41]. On the other hand, in the physical absorption case, the CO_2 can be flashed off from the CO_2-rich solvent by gradually reducing its pressure, which eliminates the need for a reboiler and an overhead condenser. Moreover, hydraulic expanders can be used to recover the power needed to recompress the separated CO_2 gas. Since the remaining carbon oxides (0.32% mol CO, 600 ppm CO_2) in the syngas after the CO_2 removal are poisonous to ammonia catalyst, part of the hydrogen produced is used to convert them into inert methane in a methanator [38].

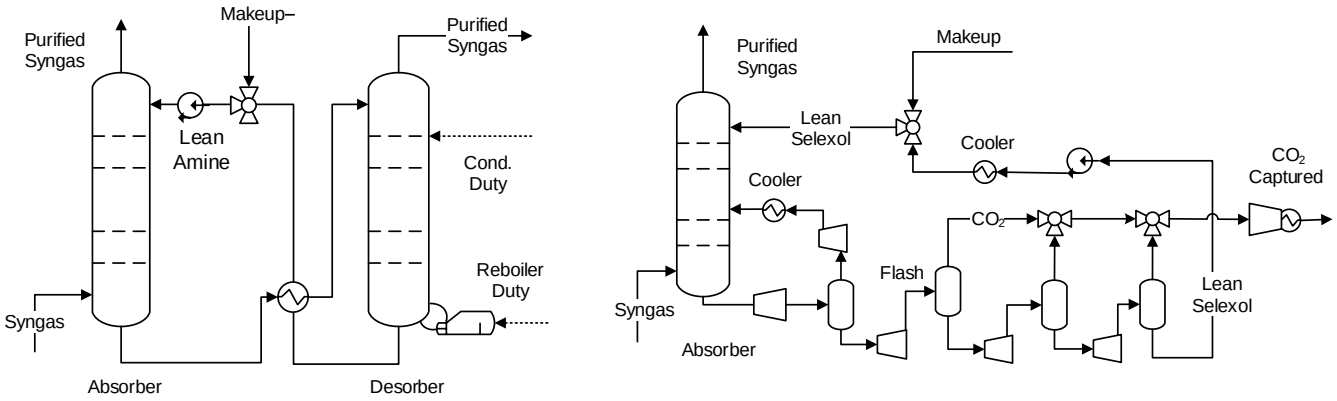

Fig. 2. Chemical (left) and physical (right) absorption carbon capture systems.

Finally, the syngas is compressed above 150 bar and fed to an ammonia synthesis loop composed of an exothermic reactor and a condensation-separation system. Higher nitrogen conversion per pass (10-30%) can be achieved by controlling the inlet temperature of three sequential catalytic beds, where the reaction (R.3) takes place [42]:

$$N_2 + 3H_2 \rightarrow 2NH_3 \qquad \Delta H^o_{298} = -92\ kJ\ mol^{-1} \qquad \text{R.3}$$

The reactor performance and, consequently, the loop efficiency are affected by the reactor operation conditions (feed pressure, temperature and composition, heat removal and catalysts design), as well as by the amount of inerts (i.e., argon, methane, water) and ammonia recycled. Thus, in order to avoid the build-up of inerts and keep them down to an acceptable level, a continuous withdrawal of a portion of the hydrogen-rich recycled stream is performed [38]. This is suitably achieved after the ammonia bulk removal and before the fresh syngas addition, i.e. where inert content is higher [43]. Finally, since ammonia condensation is not completely satisfactory by only using water or air cooling, the ammonia-rich gas is refrigerated to -20°C by using a vapor compression refrigeration system.

2.2. Utility systems

In order to achieve the reforming process, natural gas is not only consumed as both feedstock in the reformer and but also to produce an expensive, high-grade hot utility in a natural gas-fired furnace equipped with combustion air preheating. It is worthy to notice that, since the flue gas must be cooled down to the stack temperature, some of its exergy heat may be available below the pinch temperature, representing so an increase in the cold utility consumption and, thus, an avoidable loss. For this reason, two different scenarios should be considered. The first one consists of a direct competition of the combustion gas with the steam network for providing the hot utility streams required at lower temperatures. Alternatively, the hot fumes could be used to preheat the combustion air by using the excess heat exergy available below the pinch point. In this way, the air preheating defines a cold stream whose target temperature is equal to the utility pinch point. The effect of air preheating is an increase of the adiabatic combustion temperature, which translates into an increase of the heat exergy available at high temperature [44]. Actually, the reactants preheating could be interpreted as a chemical heat pump [45]. Meanwhile, a mechanical draft cooling tower and a vapor compression refrigeration system together with a mechanical vapor recompression (MVR) process supply the

cooling and heat pump requirements of the whole plant. Cooling water inlet and outlet temperatures are set as 40°C and 25°C, respectively, and a cooling tower power-to-cooling duty ratio of 0.021 kW_{el}/kW_{th} is assumed [46]. The refrigeration and heat pump systems are defined in terms of their representative exergy efficiency (50%) as shown in Eqs.(1-6):

$$\begin{aligned} COP_{\text{refrig, actual}} &= \eta_{ex} \cdot COP_{\text{refrig, Carnot}} \\ &= \eta_{ex} \cdot T_{evap} \Big/ \left(T_{cond} - T_{evap} \right) \end{aligned} \tag{1}$$

$$W_{r\,\text{refrig}} = \frac{\dot{Q}_{evap}}{COP_{\text{refrig, actual}}} \tag{2}$$

$$\dot{Q}_{cond} = \frac{\dot{Q}_{evap} \cdot \left(COP_{refrig,actual} + 1 \right)}{COP_{refrig,actual}} \tag{3}$$

$$\begin{aligned} COP_{\text{heatpump, actual}} &= \eta_{ex} \cdot COP_{\text{heatpump, Carnot}} \\ &= \eta_{ex} \cdot T_{cond} \Big/ \left(T_{cond} - T_{evap} \right) \end{aligned} \tag{4}$$

$$W_{heatpump} = \frac{\dot{Q}_{cond}}{COP^{HP}_{heatpump,actual}} \tag{5}$$

$$\dot{Q}_{evap} = \frac{\dot{Q}_{cond} \cdot \left(COP^{HP}_{heatpump,\ actual} - 1 \right)}{COP^{HP}_{heatpump,\ actual}} \tag{6}$$

On the other hand, the steam network superstructure is composed of a set of superheated steam headers and draw-off levels of steam (Fig.1) that allows for the recovery and distribution of the waste heat along the chemical plant. The choice of the optimal levels of steam is performed by inspecting the profile of the grand composite curve (GCC) of the chemical process [47]. Thus, the power can be generated by optimally profiting the thermodynamic potential of the waste heat exergy via backpressure and extraction-condensation turbines. Moreover, as long as electricity can be imported from the grid, the trade-off between the additional fuel consumption and the electricity purchase to supply the power demand of the whole plant will be strongly influenced by the performance of the cogeneration and waste heat recovery systems, as well as by the ratio between the electricity and the natural gas costs. This reasoning also applies to the suitability of the integration of a gas turbine system with regeneration, aiming to increase the cogeneration efficiency [48]. Finally, in the mechanical vapor recompression systems (MVR) shown in Fig. 1, the enthalpy of condensation of a compressed stream is used to boil up the column bottom, instead of consuming a high-grade utility stream (e.g. steam). According to some authors, the power consumed by the MVR can be as small as 10-15% of the boiling or condensation duty (in an energy basis) [161].

3. Methodology

A methodology based on the combination of the exergy method [49] and the energy integration [50] is used to assess the performance of the various components of the integrated syngas and ammonia production plant operating with three different carbon capture configurations. In the following, the procedure proposed for integrating the reactor profile to the remaining energy systems is presented. Next, the optimization problem for calculating the minimum energy requirement and minimum operating cost is defined. Finally, the exergy indicators used for estimating the performance of each configuration, which allow performing systematic comparisons between different designed setups, are proposed.

3.1. Process modeling

The complex mass and energy interactions between the multicomponent chemical systems in the ammonia production plants are analyzed by using Aspen Plus® v8.8 software and the semi-empirical Peng-Robinson-Boston-Mathias equation of state and the Redlich-Kwong with Soave modifications. In the case of the chemical absorption unit, the Electrolytic Non-Random Two Liquid (ENRTL-RK) method is used for taking into account the strongly non-ideal liquid properties, Henry components and the dissociation chemistry present in the reactive absorption-desorption systems. Moreover, in order to assess the thermodynamic properties in the physical absorption system, the perturbed chain statistical associating fluid theory (PC-SAFT) is adopted.

3.1.1. Energy integration profile of endothermic and exothermic reactors

The waste heat available below the pinch may become available above the pinch through the preheating of the reactants, which results in an increase of temperature at the reactor outlet (e.g. gas turbine combustors, ATRs, furnaces, etc.). The reaction-driven components represent the most important energy conversion systems among the chemical process as they transform the raw materials into value-added products. Indeed, the reactors fundamentally determine the design and performance of the remaining unit operations [51, 52], and the chemical reactions rates and equilibrium conversions are interrelated with the heat recovery and transport rates. Thus, the reactor performance is directly related to the balance of steam and power generation, which directly affects the energy consumption profile. Actually, reactors are responsible for the lion's share of exergy destruction among all the chemical production processes. In typical 1000 t/day ammonia plants, up to 120 MW of heat must be dissipated through the cooling water, either for enhancing the reactor yield or due to safety and reliability issues.

For this reason, an adequate representation of the *T vs. H* profile within any chemical reactor susceptible to energy integration is necessary [35]. This becomes especially true when trying to identify the opportunities for energy recovery and combined heat and power production. However, the reactor profiles are often neglected or misinterpreted, as discussed by Glavic et al. [53]. Most of the energy integration analyses only consider the reactor feed and effluents as simple cold or hot process streams that need to be heated up to (or cooled from) a representative reactor temperature. For instance, some studies arbitrarily assume that the temperature and duty in the radiant furnace is

constant, thus simplifying the integration problem of an endothermic reactor into a threshold problem that presents only cooling requirements [54]. This clearly ignores the existence of a reaction-driven *chemical utility* that should be adequately integrated along with other hot and cold utility streams, so that the overall energy consumption in the system can be minimized [55]. Previously, some authors [56] suggested decoupling the contribution of the reaction enthalpy and the heat actually transferred. The endothermic reactor was virtually coupled with a fictitious heat exchange that allowed calculating the feed preheating and the reaction enthalpy separately. However, depending on the extent of the endothermic duty required, that approach may lead to the calculation of an infeasible fictitious temperature profile that fail to represent the reactor performance in an energy integration process. Other studies [57, 58], which decompose the reformer unit into its representative components (i.e. fuel-steam mixing, reforming, heat transfer and combustion), have found that, in order to reduce the irreversibility, the temperatures of the hot utility (combustion gases) and the reformed mixture must be better matched. It can be achieved by using more or less excess air, which eventually creates a trade-off between the exergy destruction in the combustion process or in the waste heat recovery system [58].

According to Fig. 3, the reactor unit can be thermodynamically decomposed into its functions in order to better approximate the detailed *T-H* profile on the inside thereof. The reactor functions can be listed as the (i) development of the reaction enthalpy (release or absorption of chemical energy); (ii) transfer of the reaction enthalpy to the products; (iii) heat transfer from (to) the hot (cold) products to (from) the fresh reactants; and (iv) exchange between the reactor and the surroundings[53]. In this way, by successfully integrating the reactor profiles to the remaining energy conversion systems, neither the heat recovery opportunities nor the alternatives for the reduction of irreversibility will remain hidden or missing.

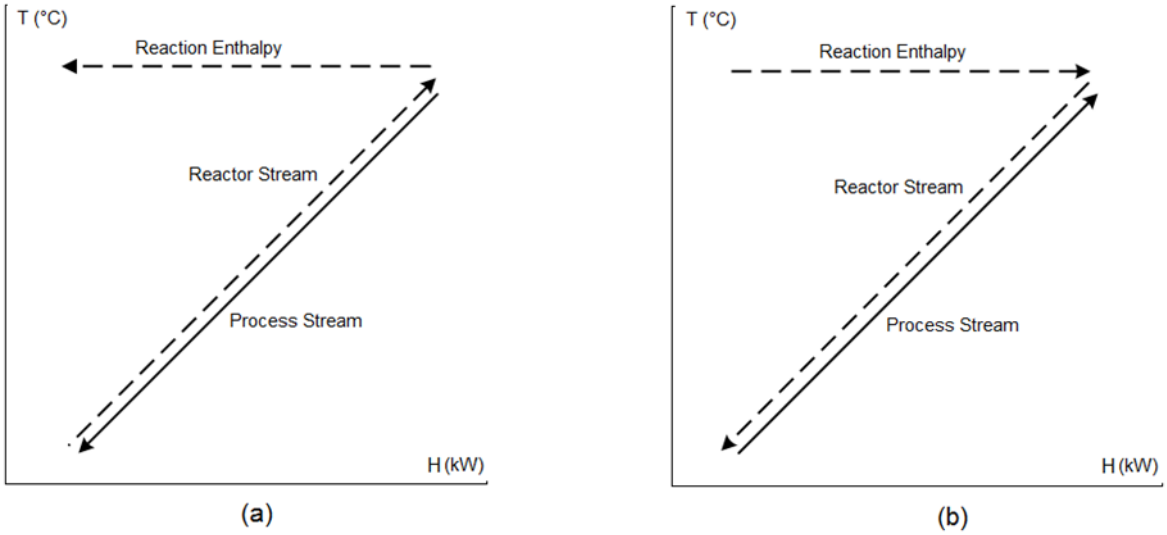

Fig. 3. Thermodynamic decomposition of chemical reactors for energy integration purposes: (a) endothermic, (b) exothermic reactor. Adapted from [53].

Figure 4 depicts the strategy used for the determination of the endothermic reactor profile in which the arrows indicate the direction of the heat transfer. The reactor feed is initially heated up to the reactor *inlet* temperature (T_{in}). Then, the mixture is assumed to virtually attain the overall reactor outlet condition ($T_{out,global}$). However, due to the endothermic nature of the system, the temperature falls down to an intermediate temperature ($T_{rxn,bed,i}$) standing for the reaction temperature that the mixture would attain if no additional heat would be supplied to continue the endothermic reaction. Only then, the reactive mixture is allowed to perform an *isothermal* endothermic reaction that increases the enthalpy of the reactants proportionately to the reaction enthalpy at the operating temperature ($T_{rxn,bed,i}$). After this partial conversion process has been achieved, the remaining reactive mixture repeats the aforementioned procedure until the global reactor outlet temperature and composition is attained.

The described approach allows decoupling the reaction and heat transfer processes and can be extended to calculate the optimal temperature profile of the reactor that reduces the irreversibility along thereof. It is worthy to notice that, by decomposing the reformer in its thermodynamic functions, the whole resembles a series of prereformer units with reheating. This scheme helps identifying the potential energy savings in the reformer duty. For instance, this approach may be helpful in deciding whether using hot gas effluents from the secondary reformer to heat the primary reformer tubes (Gas Heated Reformer concept, GHR), thus reducing the consumption of natural gas [59, 60].

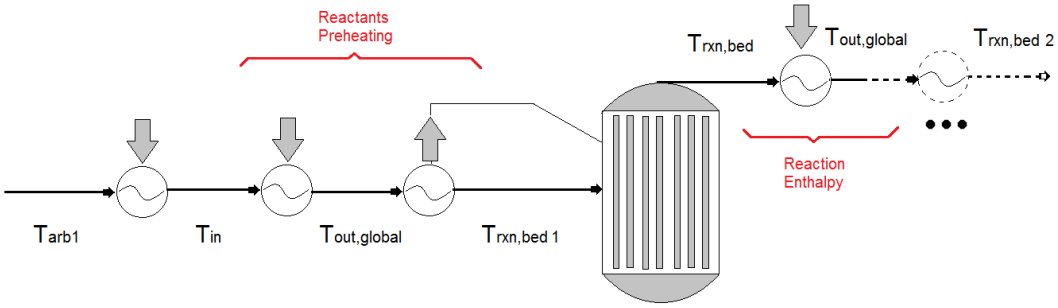

Fig. 4. Determination of the T-H profile for an endothermic reactor.

Figure 5 compares the traditional (coarse) and the proposed representation of the endothermic reformer [34]. The coarse reactor profile considers the reactor feed stream as a cold stream (580°C) required to be preheated up to the reactor operating (outlet) temperature (approx. 790°C). Next, the reaction is assumed to evolve isothermally while consuming the reaction enthalpy required by the reforming process. The total enthalpy of reaction is the same that the actual reformer and, thus, the energy requirement of the process is satisfied. However, many integration shortcomings may come about when the reactor profile is aimed to be integrated (heated) by using, for instance, a lower-grade temperature source (e.g. the waste heat from the plant).

In contrast, when a detailed profile is represented, it allows for a better approximation of the operating conditions throughout the reactor. It also helps to analyze the effect of the main reactor parameters (e.g. temperature, composition, conversion, etc.) on the whole process integration, since the reaction temperature can be considered as a decision variable [51]. Interestingly, an endothermic reactor can be compared with a heat engine in which a portion of the high temperature exergy heat provided by the

fuel is chemically converted into ‘shaft’ work (or embodied exergy into the reformed mixture), while the remaining fraction is irremediably destroyed [53].

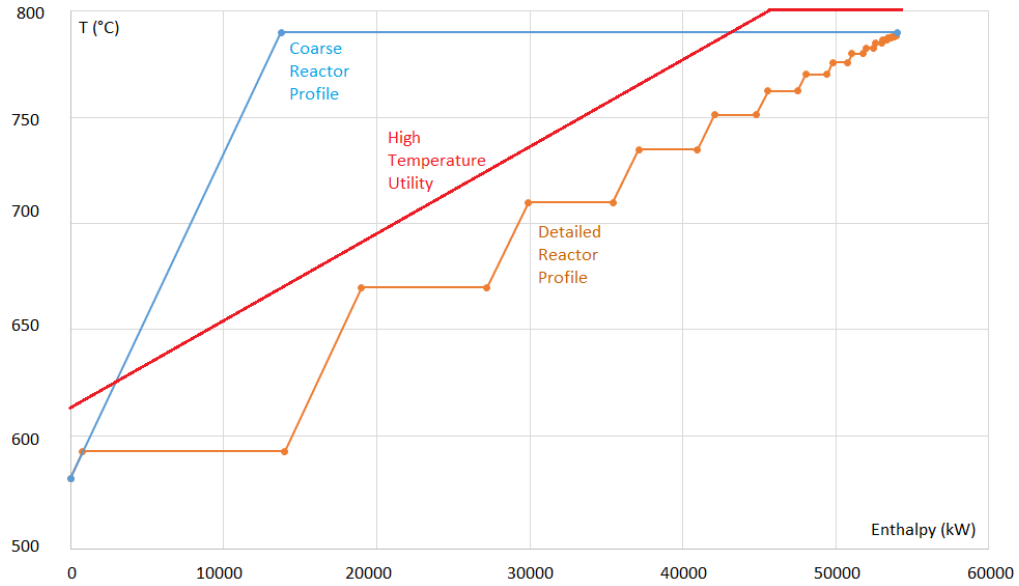

Fig. 5. Coarse and detailed representation of an endothermic reactor: T-H profile.

Analogously, the exothermic adiabatic reactor (Fig. 6) can be considered as a heat pump wherein the mechanical work input is equivalent to the *chemical work* (i.e. the variation of the chemical exergy of the reactants), which increases the physical exergy of the reactor product [26, 53]. In this way, the exothermic reactor differs in the representation of the endothermic reactor, since now the *chemical utility* provides a ‘free-ride’ (or internal preheating) to the process stream.

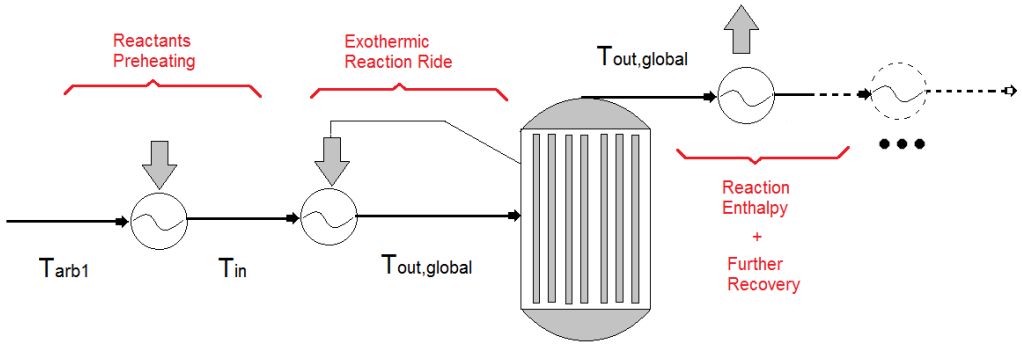

Fig. 6. Determination of the T-H profile for an exothermic reactor.

Finally, the last step of the integration of the reactor profile consists of the determination of the best alternative to recover as much as possible the enthalpy of reaction embodied in the reactor effluent. For the sake of comparison, the reaction enthalpy of the ammonia synthesis is about 8.8% (2.718 MJ/t_{NH3}) of the total energy consumption of the integrated ammonia production plant [42], which clearly renders mandatory the recovery of this excess heat.

3.2. Optimization problem definition

As it has been exposed hitherto, ammonia production plants are designed in complex formats where processes streams are integrated through recycle loops and an extensive heat recovery network. Indeed, were it not for a suitable methodology that systematically deals with the process synthesis and optimization, the determination of the best configurations may become an overwhelming, not to say impossible task in a reasonable time frame. For this reason, the selection among a set of proposed utility units (Fig. 1) of the most suitable alternatives that minimize the operating cost and the energy requirements is better addressed through the solution of a mixed integer linear programming (MILP) problem. This framework enables the reshaping of the composite curve of the chemical process, so that the operating cost of the ammonia production and the process irreversibility can be reduced.

3.2.1. Minimum energy requirement

In order to calculate the minimum energy requirement (MER), the contribution of each hot and cold streams to the overall heat balance is combined into the respective hot and cold composite curves [61]. These composite curves are shifted away from each other through a physical constraint, namely the minimum temperature approach ΔT_{min}, so that reasonable heat transfer rates can be ensured. Clearly ΔT_{min} will depend on the nature of each stream [50]. Equation (7-9) shows the optimization problem set to find the MER:

$$\min_{R_r} R_{N_r+1} \tag{7}$$

Subject to

Heat balance of each interval of temperature r

$$\sum_{i=1}^{N} Q_{i,r} + R_{r+1} - R_r = 0 \qquad \forall r = 1 .. N \tag{8}$$

Feasibility of the solution

$$R_r \geq 0 \tag{9}$$

where N is the number of temperature intervals defined by considering the supply and the target temperatures of the entire set of streams; Q (kW) is the heat exchanged between the process streams ($Q_{i,r} > 0$ hot stream, < 0 cold stream) and R is the heat cascaded from higher ($r+1$) and to lower (r) temperature intervals (kW).

3.2.2. Minimum operating cost

In order to calculate the minimum operating cost of the ammonia plant, the modeling of the process flowsheet is separated from the heat integration problem, so that the calculation of the mass and energy balances and the complex energy conversions can be handled by the process modeler Aspen® Plus [62]. Meanwhile, the determination of the minimum energy requirements (MER) and the solution of the energy integration problem is performed by using the OSMOSE Lua platform developed by the IPESE group at the École Polytechnique Fédérale de Lausanne, Switzerland [63]. Thus, the first step consists in the identification of a list of all the suitable utility systems [ω = steam network, furnace, refrigeration system, heat pump, cogeneration system, etc.] based on the analysis of the shape of the grand composite curve (GCC) [47]. Then, the computational framework manages the data transfer with the ASPEN Plus® software and builds the mixed integer linear programming (MILP) problem described in the Eqs.(10-14).This optimization problem minimizes the resources consumption (water,

natural gas and electricity) and, thus, the operating cost of the chemical plant while satisfying the constraints of the MER problem [61]. In other words, the optimization problem consist of finding the integer variables, y_w, associated to the existence or absence, and the corresponding continuous load factor, f_w, of the utility system and resource ω that minimizes the objective function given by Eq.(10):

$$\min_{\substack{f_\omega,\ y_\omega \\ R_r, W}} \left[\begin{array}{r} \left(f_\omega \cdot B \cdot c\right)_{NG,\,feedstock} + \left(f_\omega \cdot B \cdot c\right)_{NG,\,fuel} + \left(f_\omega \cdot V \cdot c\right)_{H_2O} + \left(f_\omega \cdot W \cdot c\right)_{net,\,power}^{import} \\ - \left(f_\omega \cdot B \cdot c\right)_{NH_3} - \left(f_\omega \cdot \dot{m} \cdot c\right)_{CO_2} \end{array} \right] \cdot t_{OP} \qquad (10)$$

Subject to:

Heat balance at the temperature interval r

$$\sum_{\omega=1}^{N_\omega} f_\omega q_{\omega,r} + \sum_{i=1}^{N} Q_{i,r} + R_{r+1} - R_r = 0 \quad \forall r = 1 \,..\, N \qquad (11)$$

Power balance consumed and produced

$$\sum_{\omega=1}^{N_\omega} f_\omega W_\omega + \sum_{\substack{chemical \\ units}} W_{net} + W_{imp} - W_{\exp} = 0 \qquad (12)$$

Existence and load of the utility unit w

$$f_{\min,\omega} y_\omega \le f_\omega \le f_{\max,\omega} y_\omega \quad \forall \omega = 1 \,..\, N_\omega \qquad (13)$$

Feasibility of the solution (MER)

$$R_1 = 0, \;\; R_{N_r+1} = 0, \;\; R_r \ge 0; \;\; W_{imp} \ge 0, \; W_{\exp} \ge 0 \qquad (14)$$

where N_w is the number of units in the set of utility systems; B is the exergy flow rate (kW) of the resources going in and out of the plant; c stands for the purchasing cost or the selling price (euro per kWh, m3 or kg) of the feedstock and electricity consumed or the marketable ammonia and CO_2 produced; V is the flowrate of water consumed (m^3/h); q is the heating/cooling rates supplied by the utility systems (kW); t_{OP} is the operation time (h); and W is the power produced by either the utility systems, the chemical operation units or imported from/exported to the grid (kW). It is important to emphasize that the process modeling and simulation of the chemical plant alone, including its mass and energy balances, is performed by using Aspen ® Plus software. Meanwhile, the utility units shown in Fig. 1 are modeled via equation-oriented subroutines written in the Lua programming language. Therefore, the additional equations required for the mass and energy balances of those units rely on the concept of layer (water, natural gas, ammonia, power, carbon dioxide, etc.) as shown in Fig. 7.

For instance, according to Eq.(12), the overall power generated by the utility systems (steam or gas power cycles) should be able to supply the demands of the chemical plant and other utility units (refrigeration, heat pump, cooling tower). Otherwise, the balance of the respective layer includes the possibility of importing electricity from the grid. Moreover, if a surplus of power could be produced at expense of the waste heat exergy available through all the plant, the excess electricity could be sold to the grid, provided that the electricity export is economically attractive. Analogously, in the layer of natural gas (or other resource), the amount of energy supplied by the vendors is balanced with the fuel or feedstock consumption by the chemical plant and utility systems (gas turbine, furnace). In this way, not only the balances of the resources consumed (power, natural gas, water, etc.) and the products and byproducts produced (ammonia, syngas, hydrogen, CO_2, etc.), but also of the waste heat recovered, can be performed (Fig. 7). To this end, representative market cost for the water (3.69 euro/m^3) and natural gas consumed (0.032 euro/kWh), as well as the selling prices of ammonia (0.098 euro/kWh) and CO_2 (0.0084 euro/kWh) produced are taken from literature [64-66].

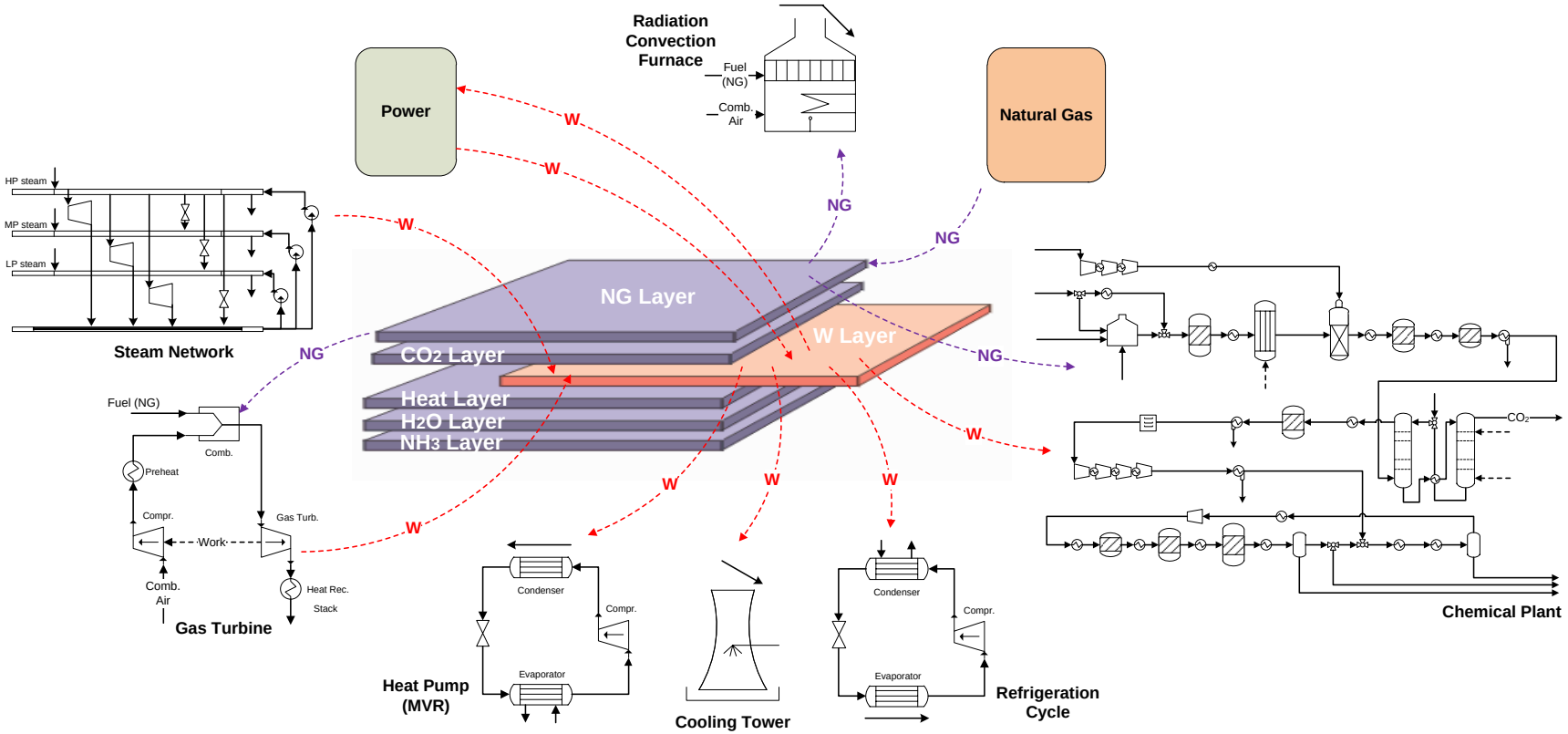

Fig. 7. Definition of the layer concept used in the optimization of the superstructure of the resources and utility systems.

3.2.3. Exergy efficiency definition

The combination of the First and Second Laws of Thermodynamics led to the concept of *exergy*, which is defined as the maximum work that can be obtained by means of reversible processes from a thermodynamic system that interacts with the components of the environment (P_o = 1atm,T_o=298.15 K) until the dead state equilibrium is attained [49]. Since exergy can be considered as a measure of the departure from the environmental conditions, it serves not only for defining indicators to assess the performance of chemical processes, but also as an indicator of environmental impact.

In this work, a methodology based on the combination of the exergy method [49] and the energy integration [50] is used to assess the performance of the various components of the integrated syngas and ammonia production plant, operating under different carbon capture configurations. Exergy indicators are used for estimating the performance of each configuration, whereas some graphical representations allow performing systematic comparisons between the different setups. Table 1 compares the *rational* exergy efficiency, Eq. (15), with the relative exergy efficiency definition, Eqs.(16), proposed for evaluating the overall performance of ammonia production plant [39]. It must be noticed that, the rational exergy efficiency is expected to be higher than the relative one as it accounts for the outlet exergy of other byproducts (CO_2, purge gas).

Table 1. Plantwide exergy efficiency definitions of the ammonia production plants.

Definition	Formula	Equation
Rational	$\eta_{\text{Rational}} = \frac{B_{useful,output}}{B_{input}} = 1 - \frac{B_{Dest}}{B_{input}} = 1 - \frac{B_{Dest}}{B_{CH_4} + B_{BFW} + W_{Net}^{Import}}$	(15)
Relative	$\eta_{\text{Relative}} = \frac{B_{consumed,\,ideal}}{B_{consumed,\,actual}} = \frac{B_{Ammonia}}{B_{CH_4} + B_{BFW} + W_{Net}^{import}}$	(16)

B = exergy rate or flow rate (kW), BFW = boiler feedwater, Dest = destroyed.

4. Results and discussion

In this section, some graphical representations, proven to be fundamental tools in the optimal choice of the most suitable energy technologies and resources consumed, are examined. Henceforth, the solution of the optimization problems for the minimum energy requirement and operating cost are discussed. Finally, the summary of the main exergy consumption remarks is presented.

4.1. Energy Integration and Minimum Energy Requirements

Figures 8a-c show the composite (CC) and grand composite (GCC) curves of the chemical process of syngas and ammonia production, operating under three different carbon capture technologies, namely MDEA, DEA and DEPG absorption systems. The minimum heating and cooling requirements, calculated by solving the optimization problem, Eqs.(7-9), are also indicated.

A first inspection of the GCC curves evidences a marked shift of the pinch point temperature from about 120ºC in the chemical absorption based (MDEA, DEA) configurations to about 500ºC in the case of DEPG-based absorption system. The shape of the curves shown in Fig. 8c is inherent to the absence of the reboiler duty in a physical absorption-based syngas purification unit. This characteristic entails particular opportunities for the integration of the utility systems and demands an appropriate approach in order to fully exploit the thermodynamic potential of the excess heat available throughout the chemical plant. Among the most interesting opportunities is the reduction of the furnace fuel consumption by preheating the combustion air along with the enhancement of the cogeneration potential. Additionally, as the process steam generation occurs below the pinch temperature in Fig.8c, the use of heat recovery steam generators (HRSG) is preferable to the utilization of auxiliary fired boilers. Otherwise, the consumption of a high temperature utility source below the pinch temperature will lead to an avoidable increase of the cooling requirement and fuel consumed. Accordingly, reduced cooling (18-23%) and heating (40-51%) requirements are expected when physical solvents are used for carbon capture purposes compared to chemical absorption-based configurations.

In the cases of ammonia plants with amine-based purification units (Figs. 7.3a-b), the reboiler and condenser streams in the desorption column generate a plateau-like pinch point at low temperatures. The desorption process demands an appreciable amount of hot utility, approx. 3.17 and 3.69 MJ/kg_{CO2} for the MDEA and DEA technology, respectively. For this reason, the installation of a mechanical vapor recompression (MVR) unit, which transfers heat across the pinch temperature by using the power generated by the power generated by the cogeneration system, seems to be a suitable energy integration approach that might help reducing the demand of the high temperature utility. According to Figs.8a-c, the target would consist of exploiting the opportunity of reactants preheating while avoiding excessive firing in the reformer furnace by maximizing the waste heat recovery. It is also recommendable to adjust the levels of pressure of the steam generation depending on the *self-sufficient* zones depicted in the GCC, and to reduce the surplus steam generation whenever it is possible. As it can be seen, the GCCs shown in Fig. 8 are not only helpful in devising the most appropriate energy technologies of the utility system that better exploit the waste heat recovery of the chemical process, but also for envisaging breakthrough approaches in the chemical plant.

Fig. 8. Composite (CC, left) and grand composite (GCC, right) curves for the simulated ammonia plants with (a)MDEA-based,(b)DEA-based and (c)DEPG-based carbon capture units.

Figure 9 compares the integration profile of a feedstock saturator with that of a steam boiler. By profiting the partial pressure vaporization effect, up to 10-30% of the reforming steam can be generated through the saturator unit [56]. The saturator transforms the plateau-like profile of the vaporization process into a smoother one, thus facilitating the integration of low-grade waste heat available elsewhere in the chemical process [67]. Furthermore, by using a prereformer, the

endothermic reforming reaction can be carried out at lower temperatures, reducing the firing in the reformer duty.

In addition, by promoting the process-to-process heat exchange in the *self-sufficient* zones at higher temperatures, instead of raising low pressure steam, the energy degradation arisen with the large heat transfer driving forces can be minimized. For instance, the use of a gas-heated reformer in combination with an enriched air blown autothermal reformer may reduce the exergy destroyed at the frontend syngas production unit, while increasing the rate of carbon captured per unit of hydrogen produced.

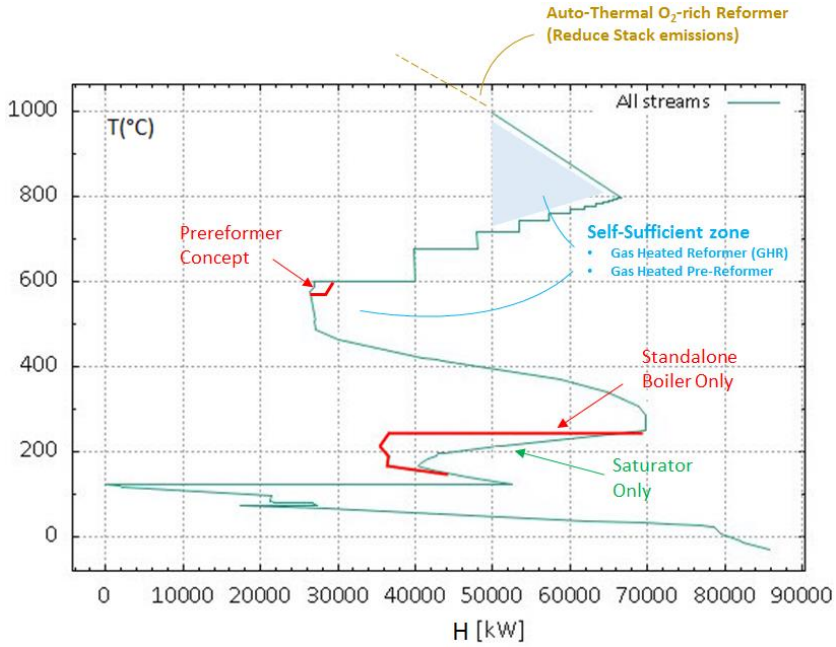

Fig. 9. T-H profile modifications by means of the incorporation of other energy technologies in the chemical system.

4.2. Minimum Operating Cost and Exergy Consumption Remarks

After performing the inspection of the GCCs presented in Section 4.1 - Figs. 8a-c, twelve optimal ammonia plant configurations are proposed and compared in terms of their exergy demands and the potential for their energy integration, when using three different carbon capture technologies (i.e. MDEA, DEA and DEPG solvent, see Table 2). They also operate under different scenarios of resources consumption and cogeneration modes (i.e. grid, mixed, and autonomous plant powered by either Rankine or Combined cycles). The most suitable utility units as well as the operating conditions thereof are determined for each configuration, and represented in Figs.10a-i, in the so-called *Integrated Curves*. Figures 10a-c show the integrated curves for the scenario in which electricity import is favored over the autonomous electricity generation in the cogeneration system (GRID mode). Since the steam superheating is hindered, the integration of a heat pump (MVR) is enabled to balance the heat demand of the chemical absorption carbon capture units. In other scenarios, Figs.10d-f, denominated MIXED mode, the steam network (0.12, 3, 40 and 110 bar, superheating 200°C) supplies a larger share of the

power consumed, but the utility system still imports an important amount of electricity from the grid in order to balance the plantwide power requirements. Differently from the GRID mode, in the MIXED mode and especially for DEPG-based ammonia plants, there is a strong incentive for recovering as much as possible the excess heat available below the process pinch (500°C) in order to increase the exergy available above it. It is also noteworthy that, in the MIXED mode, the heat pump integration is neglected by prioritizing the use of the surplus steam generated over the import of the costly electricity from the grid.

In a third scenario (AUTO mode, Figs. 10g-i), the total power consumption is entirely generated by the steam network by maximizing the waste heat recovery along the chemical plant and also consuming an important amount of natural gas. Even though this operation mode reproduces the typical conditions of modern ammonia plants [39], it is also responsible for a large amount of irreversibility associated to the cogeneration system. This problem can be thermodynamically overcome by means of the integration of a combined cycle that provides the power required by a self-sufficient ammonia plant (AUTO GT, Figs. 10k-l). Table 2 summarizes the optimal process variables calculated for the various configurations of the ammonia plant shown in Figs. 10a-l.

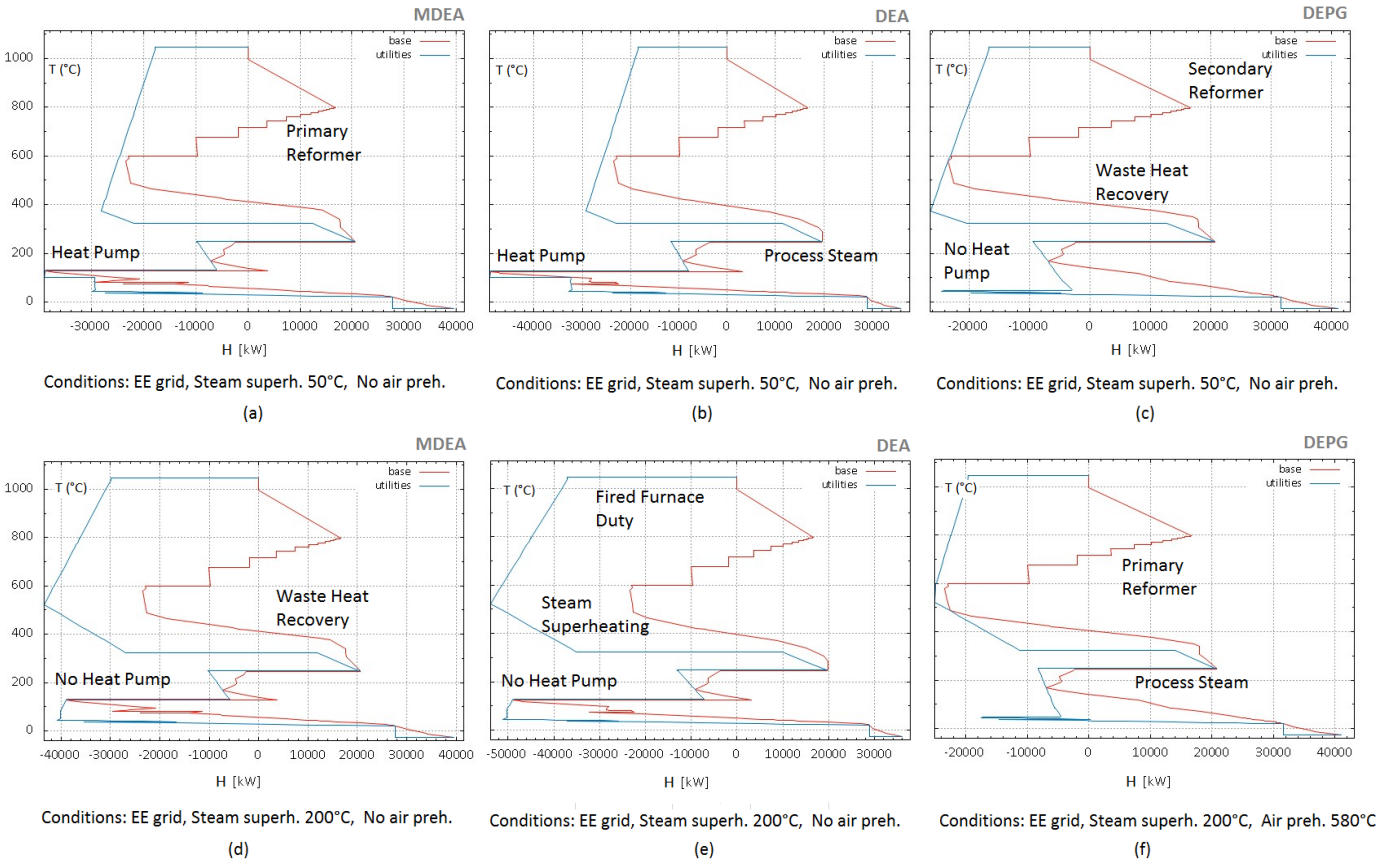

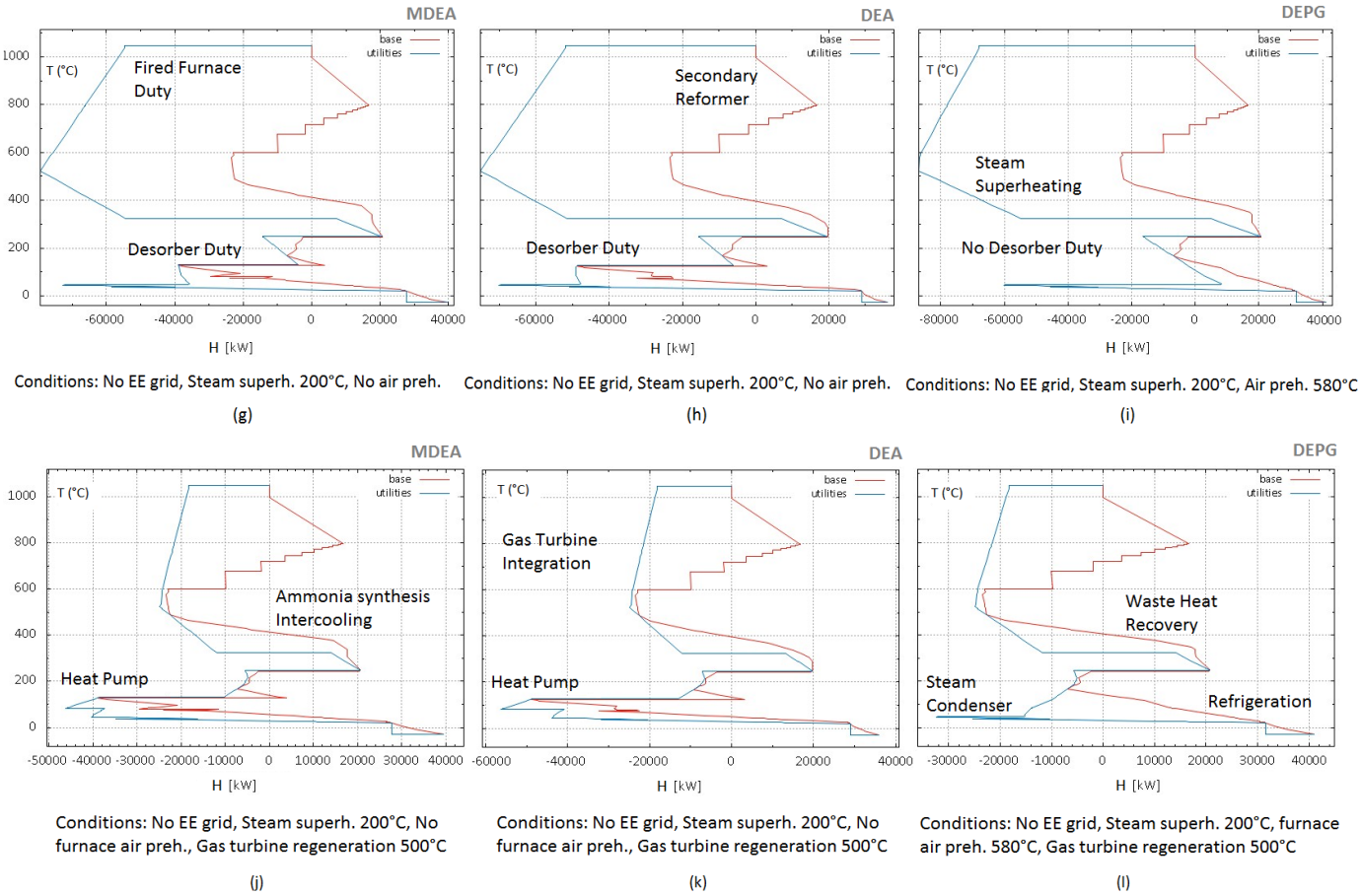

Fig. 10. Integrated Composite curves: (a-c) electricity grid import with limited steam superheating (Grid Mode), (d-f) electricity grid import with significant steam superheating (Mixed Mode), (g-i) no electricity grid import with Rankine Cycle cogeneration (Auto Mode), (j-l) no electricity grid import with Combined Cycle cogeneration (Auto GT Mode), see Table 2. EE: electricity, Superh: Steam superheating, Preh: Air Preheating.

Table 2. Optimal process variables of the studied ammonia production facilities

Process parameter	**MDEA Grid**	**MDEA Mixed**	**MDEA Auto RC**	**MDEA Auto GT**	**DEA Grid**	**DEA Mixed**	**DEA Auto RC**	**DEA Auto GT**	**DEPG Grid**	**DEPG Mixed**	**DEPG Auto RC**	**DEPG Auto GT**
Cogeneration system	Rankine	Rankine	Rankine	Combined	Rankine	Rankine	Rankine	Combined	Rankine	Rankine	Rankine	Combined
Electricity import	Yes	Yes	No	No	Yes	Yes	No	No	Yes	Yes	No	No
Feedstock consumption (GJ/t_{NH3})	23.52	23.52	23.52	23.52	23.03	23.03	23.03	23.03	23.51	23.51	23.51	23.51
Utility fuel consumption (GJ/t_{NH3})	3.28	5.50	**10.06**	7.02	3.32	6.68	9.34	6.99	3.07	**2.55**	8.83	6.21
Utility elect. grid consumption (GJ/t_{NH3})	**2.15**	1.15	0.00	0.00	2.04	**0.67**	0.00	0.00	1.90	1.71	0.00	0.00
Overall plant consumption (GJ/t_{NH3})	28.94	30.17	**33.58**	30.53	28.39	30.38	32.37	30.02	28.47	**27.76**	32.34	29.72
Extended plant consumption (GJ/t_{NH3}) [1]	33.28	33.93	**36.86**	33.52	32.59	33.82	35.53	32.96	32.58	**31.67**	35.49	32.62
Rankine cycle power generation (GJ/t_{NH3})[2]	0.44	1.25	2.46	0.72	0.43	1.47	2.18	0.66	0.53	0.70	**2.49**	0.80
Brayton cycle power generation (GJ/t_{NH3})[2]	0.00	0.00	0.00	2.01	0.00	0.00	0.00	2.02	0.00	0.00	0.00	1.63
Chemical process power demand (GJ/t_{NH3})[3]	1.61	1.61	1.61	1.61	1.61	1.61	1.61	1.61	1.81	1.81	**1.81**	1.81
Ancillary power demand (GJ/t_{NH3})[4]	0.98	0.79	0.85	1.12	0.86	0.53	0.57	1.07	0.62	0.60	0.68	0.62
Cooling requirement (GJ/t_{NH3})[5]	7.14	7.14	7.14	7.14	7.56	7.56	7.56	7.56	5.86	5.86	5.86	5.86
Heating requirement (GJ/t_{NH3})[5]	3.54	3.54	3.54	3.54	4.36	4.36	4.36	4.36	2.13	2.13	2.13	2.13
CO_2 emissions avoided (t_{CO2}/t_{NH3})	1.228	1.228	1.228	1.228	1.257	1.257	1.257	1.257	1.237	1.237	1.237	1.237
CO_2 emitted –direct (t_{CO2}/t_{NH3})	0.174	0.293	0.536	0.374	0.177	0.356	0.497	0.372	0.164	0.136	0.470	0.331
CO_2 emitted – indirect (t_{CO2}/t_{NH3})[6]	0.053	0.047	0.049	0.034	0.051	0.044	0.046	0.035	0.048	0.042	0.043	0.031
CO_2 emitted indirect – EE (%)	69.80	42.42	0.00	0.00	68.4	26.19	0.00	0.00	68.5	70.28	0.00	0.00
Total fossil CO_2 emitted (t_{CO2}/t_{NH3})	0.228	0.340	0.585	0.408	0.228	0.400	0.543	0.407	0.212	0.178	0.513	0.361
Operating Incomes[7] (euro/t_{NH3})	516.65	516.65	516.65	516.65	516.90	516.90	516.90	516.90	516.72	516.72	516.72	516.72
Operating Costs[7](euro/t_{NH3})	297.85	287.10	291.74	265.57	290.85	278.75	281.47	261.26	288.29	278.29	281.05	258.51
Operating Revenues[7](euro/t_{NH3})	218.79	229.55	224.91	251.07	226.05	238.15	235.43	255.63	228.43	238.43	235.67	**258.21**
Ammonia production (t/day)	950.36	950.36	950.36	950.36	970.45	970.45	970.45	970.45	950.84	950.84	950.84	950.84

1. Overall exergy consumption increases if the cumulative efficiency of the electricity grid (55.67%) and natural gas supply (91.09%) are considered as in ref. [68]; 2. Steam pressure levels 110, 25, 2.5 and 0.10 bar, steam superh. 200°C, Brayton cycle with regeneration, pressure ratio 20:1; 3. Power consumed by the chemical plant alone; 4. Cooling tower, heat pump and vapor compression refrigeration systems; 5. Heating requirements of the chemical processes (energy basis) determined from the composite curves; 6. It considers the indirect emissions due to the upstream supply chains of natural gas (0.0049 g_{CO2}/kJ_{CH4}) and electricity (62.09 g_{CO2}/kWh) [68, 69]; 7. Operating cost calculated as the difference between the gross operating incomes minus the operating cost by using representative prices of water, electricity, natural gas, ammonia and carbon dioxide, see section 3.2.2.

According to Fig. 11, the chemical absorption-based ammonia plant configurations present the highest overall exergy consumption figures, compared to the DEPG-based plants. Meanwhile, the lowest exergy consumption corresponds to the MIXED operating mode (partial electricity import and Rankine cycle-powered cogeneration system) by using a DEPG absorption unit (27.76 GJ/t_{NH3}). In practice, ammonia plants operate in an autonomous way in which the waste heat recovered along the plant is maximized to simultaneously produce steam and power, thus reducing the external fuel consumption. However, the AUTO (autonomous, Rankine cycle-powered) operation modes present the worst performance among all the optimized configurations due to the low cogeneration efficiency, attaining total power consumptions of about 32.27-33.5 GJ/t_{NH3}, or 21% higher than the best overall exergy consumption calculated for MIXED modes. The integration of a combined cycle (AUTO GT) partly helps to overcome this problem by increasing the cogeneration efficiency, which clearly affects the amount of fuel consumed in the AUTO operating modes (i.e. 25-30% lower). It is also worthy to notice that, when the GRID mode is adopted (i.e. limited steam superheating), the natural gas fuel consumed remains almost invariable regardless of the CO_2 capture technology used, but a larger amount of electricity is consumed instead. As already explained, this follows the integration of a mechanical vapor recompression system, restricting the fuel consumption to the supply of the high temperature reformer duty. As a conclusion, both the electricity import and the fuel consumption can be reduced by preheating the combustion air and by operating in a MIXED mode.

Fig. 11. Plantwide and extended exergy consumption and CO_2 emission figures for the various configurations studied.

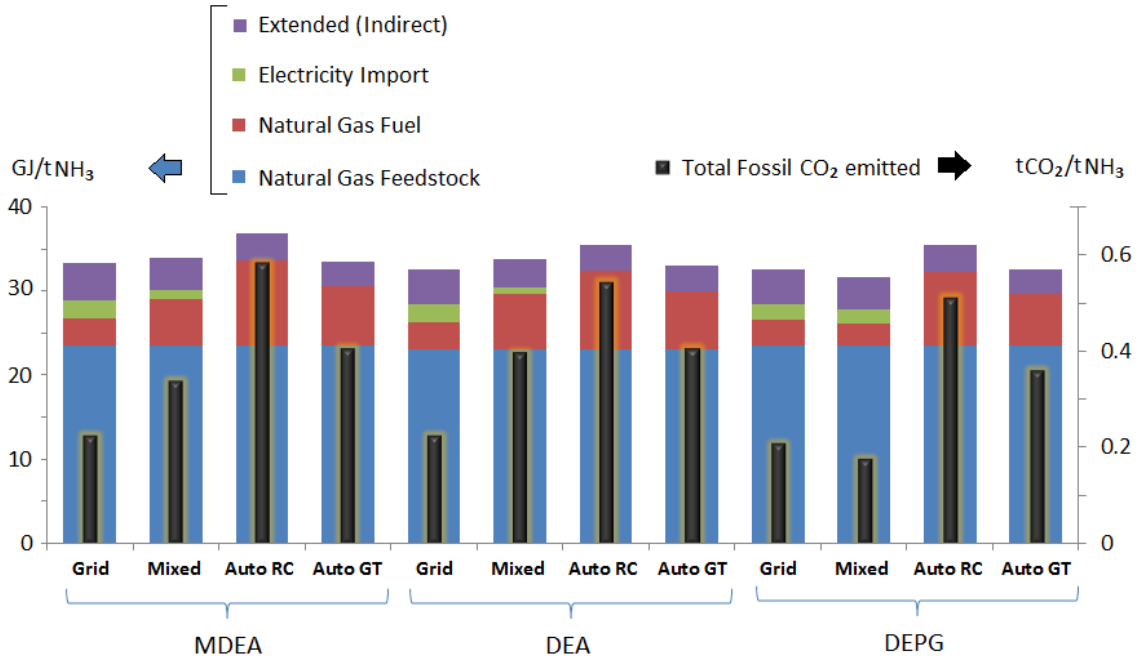

Source: Author

Additionally, Fig. 11 shows the *Extended Exergy Consumption* that takes into account the exergy efficiency of the electricity generation in the grid (55.68%) as well as of the natural gas (91.09%)

supply chain [68]. Certainly, by including the upstream inefficiencies of the feedstock supply chains into the originally standalone ammonia plant analysis, the panorama is worsened as the cumulative irreversibility further impairs the global performance of the ammonia production process. Actually, the extended exergy consumption can be 14% higher in the electricity import cases (larger cumulative losses) and 9.7% higher in the case of the autonomous configurations (cf. Table 2). Although these figures may not be immediately interesting for ammonia producers when evaluating the performance of the plant itself, they certainly prove to be useful for either issuing public and environmental policies or carrying out decision-makings that aim to holistically compare the impact of the fertilizers sector with other industrial sectors in a fair level playing field.

Table 2 also shows the indirect and direct CO_2 emissions associated to the ammonia production process. The former accounts for the emissions owed to the upstream supply chains of natural gas (0.0049 g_{CO2}/kJ_{CH4}) and electricity (62.09 g_{CO2}/kWh) as reported in ref. [68, 69]. In turn, the direct CO_2 emissions originate in the fired furnace of the externally heated primary reformer. On the other hand, the avoided CO_2 emissions are those produced along the process unit reactions and captured by either the physical or chemical absorption systems, and commercialized after its purification. As it can be observed, the contribution of the electricity generation to the indirect emissions can be as high as 70%, indicating that the impact of this resource should not be lightly neglected if a broader comparison with other alternative hydrogen and ammonia production routes (biomass, solar, nuclear and wind energy) is aimed. In spite of this, the electricity import operating modes (GRID and MIXED) are still the ones with the lowest associated overall CO_2 emissions (0.217 ton_{CO2}/ton_{NH3}). This is not surprising due to the low CO_2 footprint associated to the Brazilian electricity mix [68, 69]. Thus, the environmental impact of the ammonia production process is a strongly location-dependent industrial activity, as it has been also demonstrated by using alternative ammonia production routes from biomass gasification [21, 70, 71]. Anyway, the greater challenge will remain in the CO_2 capture from the fumes of the primary reformer furnace, as the desorption energy per ton of CO_2 is generally increased in post-combustion applications [72, 73].

In addition, according to Table 2, the lowest revenue (i.e. highest operating cost) corresponds to the MDEA absorption-based ammonia plant operating under the GRID mode. It can be partly explained by an intensive import of expensive electricity. However, it is also shown that, even if the AUTO mode with Rankine cycle effectively reduces (2-3%) the operating cost compared to GRID mode, the same cost is actually higher (1-2%) than in the MIXED mode. Thus, although the costly electricity import may actually impair the operating cost of the utility system, the overall effect can be eventually compensated by an appropriate integration of the cogeneration system as in the MIXED mode. It is also noteworthy that, regardless of the absorption solvent used for carbon capture purposes, when the ammonia plant is powered by a combined cycle (steam network plus gas turbine system), the operating cost can be reduced from 1 up to 13% compared with other configurations, either autonomous or grid-dependent. For the sake of a more complete comparison, the trade-off between the capital cost increase and the operating cost reduction (i.e. the marginal purchasing cost of an additional gas turbine system) has been roughly estimated by assuming a specific open cycle gas turbine (OGCT) cost of 900

USD/kW incl. IDC [74] or 3.6-4.5 euro/t_{NH3}. This value is less than one fourth of the total reduction (19.7-39.3 euro/t_{NH3}) of the operating costs when a gas turbine system is integrated. Then, as a preliminary estimation, there is a net gain in the revenues even at expense of the introduction of an OGCT system, because the reduction in the respective operating cost offsets its increased capital cost. In this way, the best performance in terms of total revenues still corresponds to the ammonia plant powered by a combined cycle and using DEPG as the carbon capture solvent.

Fig. 12 depicts the breakdown of the power generation and consumption amongst the main power consumers of the chemical plant as well as the ancillary utility systems (heat pump, refrigeration, cooling tower). As expected, the two largest power demands correspond to the process air and syngas compression systems, required to operate the ammonia plant at elevated pressures. The ammonia refrigeration-separation system is also responsible for about one fourth of the overall power consumption. Due to the economy of scale, higher pressures allow reducing the size of the plant components per unit of throughput of ammonia produced, as well as favors the syngas conversion and ammonia separation. However, the future trend points towards the utilization of lower reaction pressures as better catalyst with higher activities at milder operation conditions are constantly developed [42]. It must be also noticed the effect of the integration of a mechanical vapor recompression system (heat pump) on the overall power consumption of the utility systems. Namely, a considerable amount of costly electricity import and additional natural gas consumption are required when operating in either the GRID mode or the combined cycle-powered AUTO mode, respectively. In fact, the heat pump consumption is comparable to the total power produced by the Rankine cycle alone.

Finally, the highest power consumption related to the DPEG pumping must be compared to that of the amine-based systems. This is a well-known issue related to the DEPG absorption systems, i.e. the reduced heating requirement comes at expense of a higher amount of power consumed in the circulation pump [75]. Certainly, higher capture rates are desirable to avoid the consumption of the valuable hydrogen in the downstream methanator unit, also because slipped methane acts an inert in the ammonia loop, increasing the need of a larger purge. However, larger capture efficiencies with DEPG require higher solvent circulation rates, since the solvent capacity is compromised as the temperature increases [76, 77]. In fact, for a 90% CO_2 capture efficiency, the solvent/CO_2 loading ratio can be as high as 5:1, i.e. threefold the value when more stringent capture efficiencies (>95%) are imposed [78]. Meanwhile, DEA recirculation rate is set as 716 m^3/h, with maximum and minimum CO_2 loadings of 0.47 and 0.025 $kmolCO_2/kmol_{DEA}$, respectively. For the case of MDEA, those figures are set as 495 m^3/h, 0.51 and 0.013 $kmolCO_2/kmol_{MDEA}$, respectively.

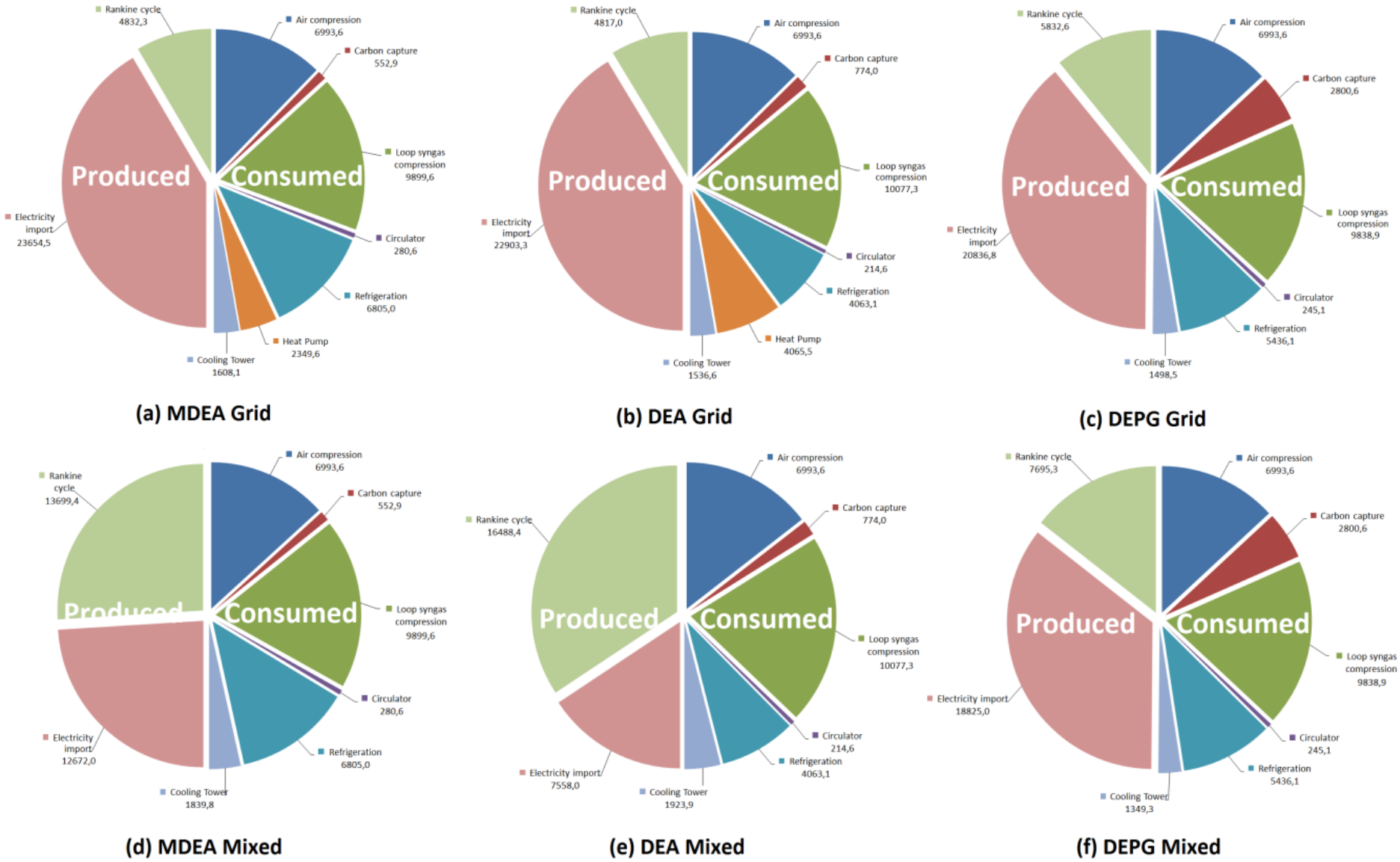

Fig. 12. Breakdown of power generation and consumption in each plant configuration shown in Table 2.

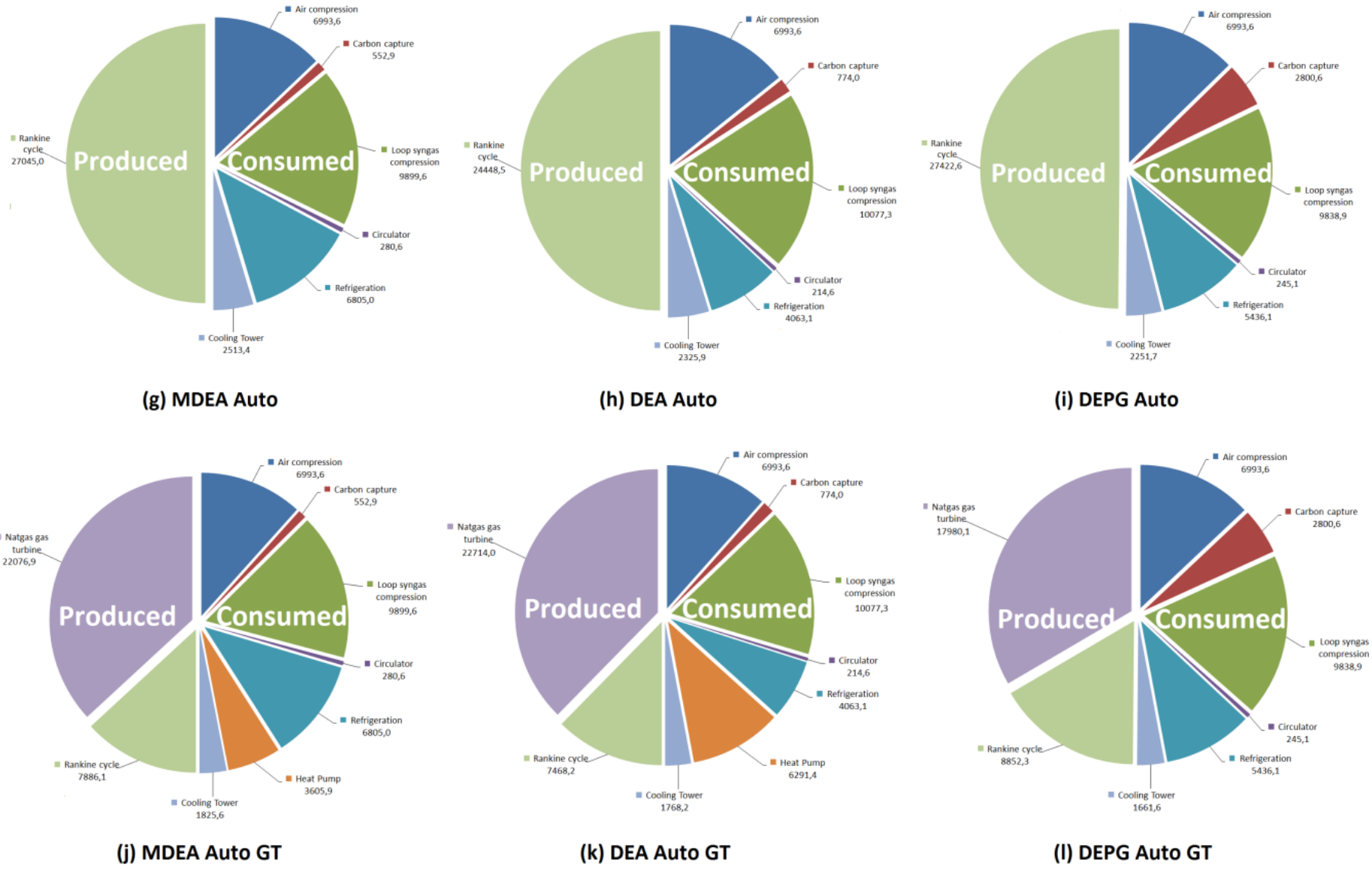

Fig. 12. Breakdown of power generation and consumption in each plant configuration shown in Table 2(Cont'd)

4.2. Exergy efficiency and Exergy Destruction Analyses

Figure 13 compares the relative and extended relative exergy efficiency of the various ammonia plant configurations and operation modes studied. As expected, the integration of a combined cycle into a traditionally Rankine cycle-based ammonia plant increases the relative exergy efficiency about 8.8%. Nonetheless, the highest relative exergy efficiency still corresponds to MIXED operation mode with physical absorption-based syngas purification unit. This behavior is closely followed by the GRID operation modes, regardless of the syngas purification system utilized. It is also worthy to notice the appreciable reduction (> 10%) of the relative exergy efficiency when a broader scope, i.e. an *extended* framework that accounts for the irreversibilities in the natural gas and electricity upstream supply chains, is considered.

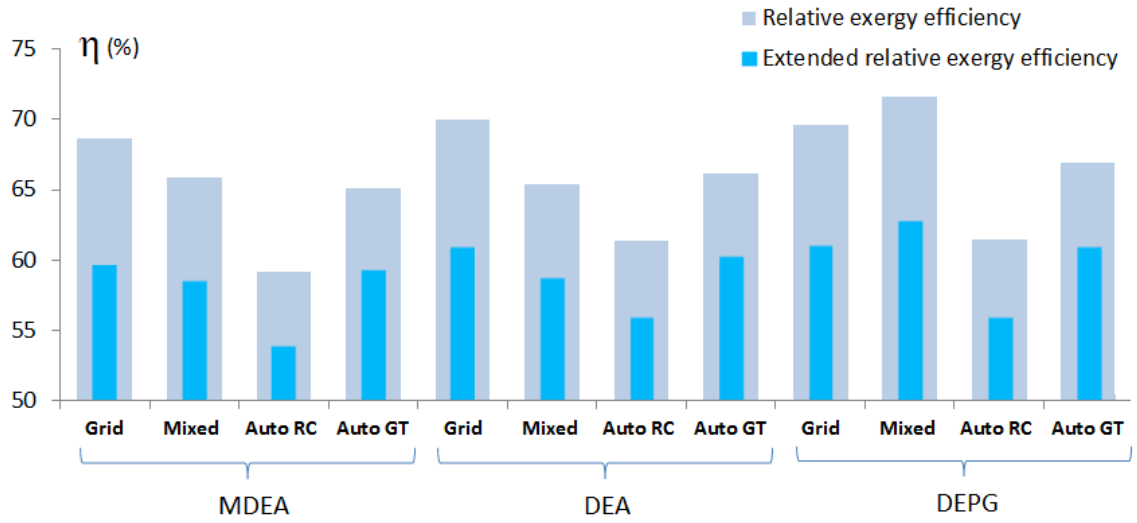

Fig. 13. Plantwide and extended exergy consumption figures for the various configurations studied.

Table 3 summarizes the exergy efficiency and the specific exergy destruction, used as indicators to rank the performance of the analyzed ammonia plant configurations. It is interesting to point out the striking reduction of the overall exergy efficiency when going from its pure *rational* definition up to the *extended relative* one. In fact, the efficiency drop can be as high as 19.3-23.8%, since this broader scope of reduction accounts for both the exergy destroyed along the upstream feedstock obtainment stages as well as for disregarding the potential utilization of the ammonia byproducts (CO_2, purge).

Within the same scope, the increase in the exergy destruction may achieve 31% in the AUTO and 39% in the AUTO GT operating modes, whereas as much as 43-77% for the GRID and MIXED operation modes. Thus, at a first glance, the higher increase in the extended exergy destruction could be wrongly attributed to the intensive utilization of the less efficient electricity mix (55.67%), if compared to the more efficient natural gas supply chain (91.09%). However, the electricity utilization still remains as the most efficient way of driving the ammonia plant configurations studied. In other words, although the electricity import entails the consumption of a relatively inefficiently produced input (i.e. grid electricity), the high-grade and readily available nature of the electricity consumed actually lead to an

improved performance of the ammonia production process, only comparable to the utilization of a combined cycle (AUTO GT) in an autonomous operation mode (Table 3, last column). This fact once again emphasizes the importance of the characteristics of the electricity mix in which the chemical process is embedded. In the hypothesis that much less efficient electricity mixes were considered, the AUTO and AUTO GT operation modes may become more attractive alternatives for electricity generation via integrated CHP systems, than importing costly, less efficiently and less environmentally friendly electricity from 'dirtier' grids.

Table 3. Exergy destruction and exergy efficiencies for the chemical and physical absorption-based ammonia production plant configurations

Process parameter	**MDEA Grid**	**MDEA Mixed**	**MDEA Auto RC**	**MDEA Auto CC**
Rational exergy efficiency (%)	78.40	75.21	67.59	74.32
Extended rational exergy efficiency (%)	68.20	66.88	61.57	67.70
Relative exergy efficiency (%)	68.67	65.87	59.20	65.09
Extended relative exergy efficiency (%)	59.73	58.58	53.93	59.29
Exergy destruction (GJ/t_{NH3})	6.25	7.48	10.88	7.84
Extended exergy destruction (GJ/t_{NH3})	10.58	11.24	14.16	10.83

1.The exergy efficiency and the specific exergy destruction change if the cumulative exergy efficiency of the electricity grid (55.67%) and of the natural gas supply chain (91.09%) are considered as in ref. [68].

Table 3. Exergy destruction and exergy efficiencies for the chemical and physical absorption-based ammonia production plant configurations (cont'd)

Process parameter	**DEA Grid**	**DEA Mixed**	**DEA Auto RC**	**DEA Auto GT**
Rational exergy efficiency (%)	79.05	73.88	69.34	74.76
Extended rational exergy efficiency (%)	68.86	66.36	63.17	68.10
Relative exergy efficiency (%)	70.00	65.43	61.41	66.21
Extended relative exergy efficiency (%)	60.98	58.77	55.94	60.31
Exergy destruction (GJ/t_{NH3})	5.95	7.94	9.92	7.58
Extended exergy destruction (GJ/t_{NH3})	10.15	11.38	13.09	10.51

11.The exergy efficiency and the specific exergy destruction change if the cumulative exergy efficiency of the electricity grid (55.67%) and of the natural gas supply chain (91.09%) are considered as in ref. [68].

Table 3. Exergy destruction and exergy efficiencies for the chemical and physical absorption-based ammonia production plant configurations (cont'd)

Process parameter	**DEPG Grid**	**DEPG Mixed**	**DEPG Auto RC**	**DEPG Auto GT**
Rational exergy efficiency (%)	79.69	81.72	70.17	76.35
Extended rational exergy efficiency (%)[1]	69.81	71.63	63.92	69.55
Relative exergy efficiency (%)	69.64	71.59	61.48	66.89
Extended relative exergy efficiency (%)[1]	61.01	62.76	56.00	60.93
Exergy destruction (GJ/ton_{NH3})	5.78	5.08	9.64	7.03
Extended exergy destruction (GJ/ton_{NH3})[1]	9.89	8.99	12.81	9.93

1.The exergy efficiency and the specific exergy destruction change if the cumulative exergy efficiency of the electricity grid (55.67%) and of the natural gas supply chain (91.09%) are considered as in ref. [68].

Figure 14 shows the exergy destruction breakdown among the most representative components of the studied ammonia plant configurations studied. As it can be seen, the primary and secondary reformers together are responsible for nearly 26-54% of the total exergy destroyed. As expected, the highest exergy destruction share of the utility systems (*others*) is attained through an intensive utilization of

both the steam network and the cogeneration systems (27-52%), e.g. in both AUTO and AUTO GT operating modes. The ammonia synthesis reactor has a contribution to the exergy destruction that may oscillates between 7.8-17.3%, which depends on the amount of inerts, the recycling ratio and conversion in the ammonia synthesis loop [79]. A marked difference exists between the shares of the exergy destruction presented by the carbon capture units analyzed. The amine-absorption carbon capture units by either using DEA or MDEA solvent are responsible for one tenth to one fifth of the total exergy destruction. Those figures are smaller when physical absorption systems are used (<4.6%). Accordingly, the use of carbon capture systems that spare energy intensive desorption processes can be effectively used to reduce the contribution of the syngas purification system to the total amount of irreversibility in the ammonia plant.

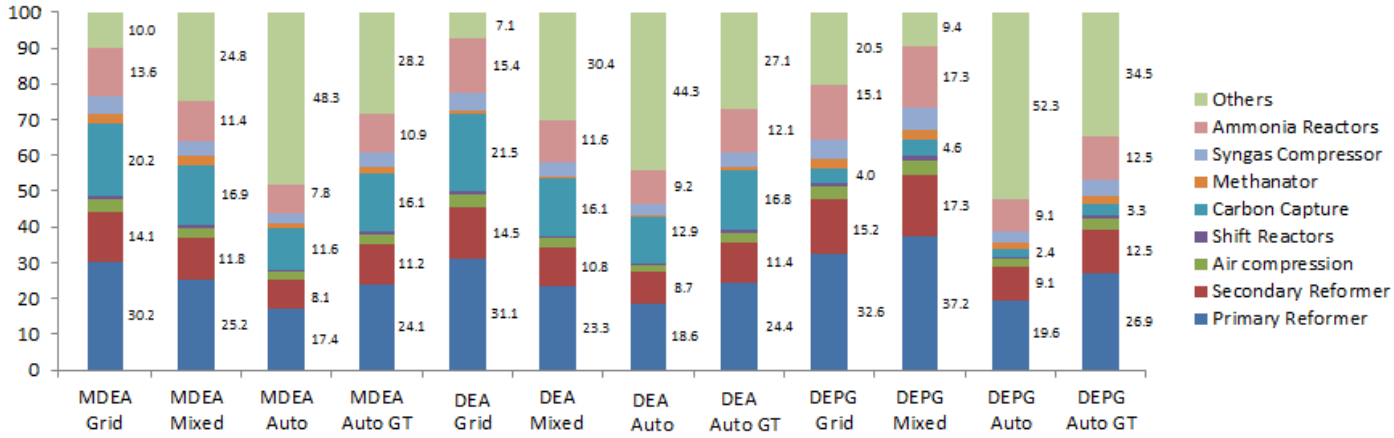

Fig. 14. Exergy destruction breakdown in each plant configuration shown in Table 2.

The difference between the irreversibility associated to the heat exchange network (HEN) of the ammonia production plants operating under the AUTO and AUTO GT modes can be graphically represented by the Carnot Integrated Curves shown in Fig. 15a-b. In this plot, the area enclosed by the curves of the utility systems and the chemical plant can be interpreted as the exergy destroyed. Thus, the closer the two curves, the lesser the irreversibility in the HEN. As expected, due to an upgraded utilization of the exergy heat of the high-grade utility produced by the fired furnace, the exergy destruction rate drastically drops when a Combined cycle is integrated to the ammonia production unit. The recovery of the exergy embodied in the high temperature flue gases is maximized by using the combustion gases to drive the gas turbine system, and only thereafter for gas turbine cycle regeneration purposes, process streams preheating or steam generation, respectively, instead of using the combustion gases for directly producing steam [80, 81].

Certainly, this modification perturbs the whole power and heat balance, particularly within the *self-sufficient zones* where the cogeneration has benefited from. In other words, since part of the excess heat exergy has been used to produce power, additional fuel consumption will be required to ensure the balance of the heating demands of the chemical process. In spite of this, the integration of a waste heat recovery steam network generally reduces the large driving forces related to the process-to-process heat exchange, even at the expense of supplementary fuel consumption. For instance, as shown in Figs.15a-b, it is preferable to generate a surplus of electricity for driving the heat pump (MVR)

system by extracting most of the thermodynamic potential in the self-sufficient zones, than directly using waste heat from the process to supply the desorption reboiler duty [82]. Roughly speaking, due to the technical and metallurgical limitations of the energy technologies considered, the use of a gas turbine system becomes advantageous when aiming to better exploit the thermodynamic potential at higher temperatures (above 500°C) whereas the steam network represents the most suitable alternative for recovering the waste heat exergy available at lower ones (300-500°C). Supercritical Rankine cycles or Graz-related power cycle may represent also interesting alternatives for utility systems with reduced exergy destruction rates and post-combustion CO_2 emissions, as long as the industrial ammonia plants investors can afford large initial capital investments.

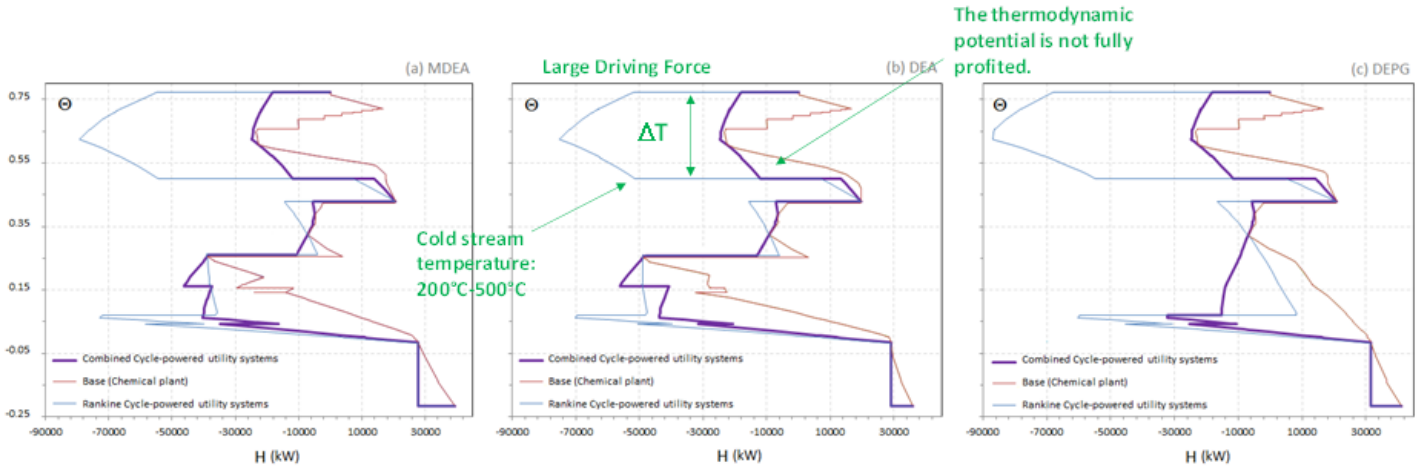

Fig. 15. Carnot integrated curves for the AUTO and AUTO GT scenarios shown in Figs. 10g-l: (a)MDEA-based, (b)DEA-based, (c)DEPG-based carbon capture ammonia plants. Θ is the Carnot factor calculated as $1-(To/T)$ *where To = 298 K.*

5. Conclusions

In this work, a systematic methodology based on a mixed integer linear programming (MILP) and modular chemical process simulation approach allows determining the most suitable utility systems that satisfy the minimum energy requirement (MER) with the lowest resources consumptions and operating cost in a highly integrated syngas and ammonia production plant. Various operating scenarios based on the utilization of three types of syngas purification systems, as well as several energy resources and cogeneration technologies have been compared in terms of exergy consumption and efficiency as well as optimal operating revenues. By using the energy integration method, the most appropriate utility systems and their operation conditions, that maximize the recovery of the thermodynamic potential of the excess heat produced along the chemical process, have been identified. This has been possible through the development a suitable representation of the energy integration profile for the reactive systems, acknowledged as the key components of the energy intensive chemical plant. Moreover, an extended exergy analysis has been performed so that a broader insight into the major sources of irreversibility can be hierarchized and the exergy destruction in the ammonia production can be reduced by proposing the utilization of better energy technologies for cogeneration.

Direct and indirect CO_2 emissions produced in the ammonia production process are also calculated, allowing for better comparisons with other industrial and chemical process in terms of their environmental impact. On the other hand, the valorization of some plant byproducts (e.g. captured CO_2) simultaneously increased the chemical plant efficiency, while mitigating its environmental burden. As a result, by operating either in a mixed mode (i.e. partial electricity import with an improved waste heat recovery and cogeneration systems) or in a totally autonomous mode with combined cycle cogeneration systems, along with the use of physical absorption syngas purification units, the process irreversibility and operating cost can be appreciably reduced, whereas the conventional plant efficiency is increased (ca. 8-10%). Thus, by considering that typical ammonia plants actually operate in autonomous modes with no other energy input that natural gas, the integration of the gas turbine system is the most rational alternative for increasing the exergy efficiency and the reduction of the operating costs in the SNF facilities.

Acknowledgments

The first author would like to thank to the Swiss Government Excellence Scholarship Program (Grant 2016.0876), and the Colombian Administrative Department of Science, Technology and Innovation - COLCIENCIAS. Second author thanks to the National Research Council for Scientific and Technological Development, CNPq (grant 306033/2012-7).

References

1.FAO. Current world fertilizer trends and outlook to 2015. 2011. Accessed Oct. 15, 2016. Available at: ftp://ftp.fao.org/ag/agp/docs/cwfto15.pdf.
2.Ribeiro, P.H., Contribution to the Brazilian Databak for supporting the Life Cycle Analysis of the Nitrogen Fertilizers [In portuguese], MSc Thesis in Polytechnic School, Department of Chemical Engineering. 2009, University of Sao Paulo.
3.PETROBRAS. Facts and Data: Understand why we invest in fertilizers [In Portuguese]. Accessed Dec. 14, 2016; Available at: http://www.petrobras.com.br/fatos-e-dados/entenda-por-que-investimos-em-fertilizantes.htm.
4.Hernandez, M., Torero, M., Fertilizer Market Situation: Market Structure, Consumption and Trade Patterns, and Pricing Behavior. IFPRI Discussion Paper 01058. International Food Policy Research Institute. January 2011
5.Dias, V., Fernandes, E., Fertilizers: A global synthetic insight. BNDES Setorial Rio de Janeiro, set. 2006, (24): p. 97-138.
6.CIESP. Fertilizers: Petrobras widens participation, May 12, 2014 [In Portuguese]. 2014. Accessed May 14, 2016; Available at: http://www.ciesp.com.br/cubatao/noticias/fertilizantes-petrobras-amplia-atuacao.
7.Portal.Brasil (2014) Producing fertilizers is strategic to [In Portuguese] Infrastrutura, Nitrogenados, May 3, 2014.
8.Worrell, E., Blok, K., Energy savings in the nitrogen fertilizer industry in the Netherlands. Energy,1994.19(2): p.195-209.
9.Kirova-Yordanova, Z. Energy Integration and Cogeneration in Nitrogen Fertilizers Industry: Thermodynamic Estimation of the Efficiency, Potentials, Limitations and Environmental Impact. Part 1: Energy Integration in Ammonia Production Plants. in 25th International Conference on Efficiency, Cost, Optimization, Simulation and Environmental Impact of Energy Systems, ECOS, 2012. Perugia, Italy.
10. Kirova-Yordanova, Z., Thermodynamic Evaluation of Energy Integration and Cogeneration in Ammonium Nitrate Production Complexes. International Journal of Thermodynamics (IJoT), 2013. 16(4): p. 163-171..
11. Kirova-Yordanova, Z., Exergy analysis of industrial ammonia synthesis. Energy, 2004. 29: p. 2373-2384.
12. Panjeshahi, M.H., Ghasemian Langeroudi, E., Tahouni, N., Retrofit of ammonia plant for improving energy efficiency. Energy, 2008. 33(1): p. 46-64.
13. Leites,I.,Sama, D., Lior, N., The theory and practice of energy saving in the chemical industry: some methods for reducing thermodynamic irreversibility in chemical technology processes.Energy,2003.28(1):p.55-97.
14. Sorin, M., Paris, J., Combined Exergy and Pinch Approach to Process Analysis Computers chem. Eng, 1997. 21(Suppl.): p. S23-S28.
15. Appl, M., Ullmann's encyclopedia of industrial chemistry, Vol.11. Chapter 2., 2012, Wiley-VCH Verlag GmbH & Co

16. Rafiqul, I.W., C., Lehmann, B., Voss, A., Energy efficiency improvements in ammonia production—perspectives and uncertainties. Energy, 2005. 30(13): p. 2487-2504.
17. Dopper, J.G., European Roadmap for Process Intensification. 2007, Ministry of Economic Affairs: Delft, The Netherlands. p. 53.
18. Canadian Fertilizer Institute, Benchmarking energy efficiency and carbon dioxide emissions. 2007, Canadian Industry Program for Energy Conservation.
19. Strait, R.B. New KBR Technologies available for revamping ammonia plants. in Nitrogen + Syngas International Conference and Exhibition. 2008. Moscow, 20-23 April.
20. Filippi, E., Davey, W., Thomas Wurzel, T. MEGAMMONIA- The Mega-Ammonia process for the new century. in AICHE Ammonia Safety Symposium. 2004.
21. Arora, P., Hoadley, A., Mahajani, S., Ganesh, A., Multi-objective optimization of biomass based ammonia production - Potential and perspective in different countries. J. Cleaner Production,2017. 148: p.363-374.
22. Ruth, M., Laffen, M., Timbario, T., Hydrogen Pathways: Cost, Well-to-Wheels Energy Use, and Emissions for the Current Technology Status of Seven Hydrogen Production, Delivery, and Distribution Scenarios Technical Report NREL/TP-6A1-46612. 2009, National Renewable Energy Laboratory - NREL.
23. Spath, P.L., Dayton, D.C., Preliminary Screening - Technical and Economic Assessment of Synthesis Gas to Fuels and Chemicals with Emphasis on the Potential for Biomass-Derived Syngas. NREL/TP-510-34929. 2003, National Renewable Energy Laboratory: Golden, Colorado. p. 160.
24. Liu, H., Ammonia Synthesis Catalysts: Innovation and Practice. 2013, Beijing: Chemical Industry Press, ISBN 978-981-4355-77-3.
25. Leveson, P.D., Thermally Coupled Monolith Reactor, U.S. Patent 20070009426. 2007, ZeroPoint Clean Technologies Inc.: United States. p. 12.
26. Hinderink, A.P., Kerkhof, F. P. J. M., Lie, A. B. K., De Swaan Arons, J., Van Der Kooi, H. J., Exergy analysis with a flowsheeting simulator—II. Application; synthesis gas production from natural gas. Chemical Engineering Science, 1996. 51(20): p. 4701-4715.
27. Nikačević, N., Jovanović, M., Petkovska, M., Enhanced ammonia synthesis in multifunctional reactor with in situ adsorption. Chemical Engineering Research and Design, 2011. 89(4): p. 398-404.
28. Sahafzadeh, M., Ataei, A., Tahouni, N., Panjeshahi, M., Integration of a gas turbine with an ammonia process for improving energy efficiency. Applied Thermal Engineering, 2013. 58(1–2): p. 594-604.
29. Greeff, I.L., Visser, J. A., Ptasinski, K. J., Janssen, F. J. J. G., Integration of a turbine expander with an exothermic reactor loop—Flow sheet development and application to ammonia production. Energy, 2003. 28(14): p. 1495-1509.
30. Grossmann, I., Mixed-integer programming approach for the synthesis of integrated process flowsheets. Computers & Chemical Engineering, 1985. 9(5): p. 463-482.
31. Papoulias, S., Grossmann, I., A structural optimization approach in process synthesis—II: Heat recovery networks. Computers & Chemical Engineering, 1983. 7(6): p. 707-721.
32. Papoulias, S., Grossmann, I., A structural optimization approach in process synthesis—I: Utility systems. Computers & Chemical Engineering, 1983. 7(6): p. 695-706.
33. Papoulias, S., Grossmann, I., A structural optimization approach in process synthesis—III: Total processing systems. Computers & Chemical Engineering, 1983. 7(6): p. 723-734.
34. Kalitventzeff, B., Maréchal, F., Closon, H., Better solutions for process sustainability through better insight in process energy integration. Applied Thermal Engineering, 2001. 21(13–14): p. 1349-1368.
35. Marechal, F., Palazzi, F., Godat, J., Favrat, D., Thermo-Economic Modelling and Optimisation of Fuel Cell Systems. Fuel Cells, 2005. 5(1): p. 5-24.
36. EFMA, Booklet No. 1 of 8: Production of Ammonia, in Best Available Techniques for Pollution Prevention and Control in the European Fertilizer Industry, 2000: Brussels, Belgium.
37. Shumake, B.G., Abu Diab, T., Operation Hydrogen. Hydrocarbon Engineering, 2006. February: p. 43-48.
38. Maxwell, G., Synthetic Nitrogen Products: A Practical Guide to the Products and Processes, 2004, NY: Springer US.
39. Flórez-Orrego, D., Oliveira Junior, S., On the efficiency, exergy costs and CO2 emission cost allocation for an integrated syngas and ammonia production plant. Energy, 2016. 117, Part 2: p. 341-360.
40. Hou, K., Hughes, R., The kinetics of methane steam reforming over a Ni/-Al2O3 catalyst. Chemical Engineering Journal, 2001. 82: p. 311-328.
41. Polasek, J., Iglesias-Silva, G. Using Mixed Amine Solutions for Gas Sweetening. in Seventy-First GPA Annual Convention. 1992. Tulsa, OK: Texas A&M University and Bryan Research & Engineering, inc.
42. Tamaru, K., The History of the Development of Ammonia Synthesis, in Catalytic Ammonia Synthesis, J.R. Jennings, Editor. 1991, Springer US. p. 1-18.

43. Ostuni, R., Filippi, E., Skinner, G.F., Hydrogen and Nitrogen Recovery from Ammonia Purge Gas. US20130039835 A1. 2013, Ammonia Casale SA.
44. Maréchal, F., Kalitventzeff, B., Effect modelling and optimization, a new methodology for combined energy and environment synthesis of industrial processes. Applied Thermal Engineering, 1997. 17(8): p. 981-992.
45. Flórez-Orrego, D., Oliveira Junior, S., Exergy assessment of single and dual pressure industrial ammonia synthesis units. Energy, 2017. 141: p. 2540-2558.
46. Couper, J., Penney, W. R., Fair, J. R., Walas, S. M., Chemical Process Equipment (Third Edition). 2012, Boston: Butterworth-Heinemann.
47. Maréchal, F., Kalitventzeff, B., Identification of the optimal pressure levels in steam networks using integrated combined heat and power method. Chemical Engineering Science, 1997. 52(17): p. 2977-29899.
48. Keller, A., Viswanathan, S., Integrated pressurized steam hydrocarbon reformer and combined cycle process, U.S.Patent 8375725. 2013, Phillips 66 Company, Houston, TX (US): United States.
49. Szargut, J., Morris, D, Steward, F, Exergy analysis of thermal, chemical, and metallurgical processes. 1988, New York: Hemisphere Publishing Corporation.
50. Linnhoff, B., Hindmarsh, E., The pinch design method for heat exchanger networks. Chemical Engineering Science, 1983. 38(5): p. 745-763.
51. Linke, P., Kokossis, A., Alva-Argaez, A., Process Intensification, in Computer Aided Process and Product Engineering. 2006, Wiley-VCH Verlag GmbH. p. 297-326.
52. Florez-Orrego, D., Nascimento Silva, F., Oliveira Jr., S. Syngas Production with Thermo-Chemically Recuperated Gas Turbine Systems: An Exergy Analysis and Energy Integration Study. in 31th International Conference on Efficiency, Cost, Optimization, Simulation and Environmental Impact of Energy Systems - ECOS 2018, June 17th - 22nd. 2018. Guimaraes, Portugal: University of Minho.
53. Glavič, P., Kravanja, Z., Homšak, M., Heat integration of reactors—I. Criteria for the placement of reactors into process flowsheet. Chemical Engineering Science, 1988. 43(3): p. 593-608.
54. Canmet ENERGY, Nitrogen-Based Fertilizer Industry: Energy Recovery at an Ammonia Plant. Cat. No.: M154-60/4/2009E-PDF, in Pinch Analysis: For the Efficient Use of Energy, Water & Hydrogen. 2012.
55. Smith, R., Chemical Process: Design and Integration. 2005, Manchester: Wiley and Sons.
56. Godat, J., Marechal, F., Optimization of a fuel cell system using process integration techniques. Journal of Power Sources, 2003. 118(1–2): p. 411-423.
57. Hajjaji, N., Pons, M., Houas, A., Renaudin, V., Exergy analysis: An efficient tool for understanding and improving hydrogen production via the steam methane reforming process. Energy Policy,2012.42(0):p.392-9.
58. Simpson, A., Lutz, A., Exergy analysis of hydrogen production via steam methane reforming. International Journal of Hydrogen Energy, 2007. 32(18): p. 4811-4820.
59. Aasberg-Petersen, K., Christensen, T.S., Dybkjaer, I., Sehested, J., Ostberg, M., Coertzen, R.M., Keyser, M.J., Steynberg, A. P., Chapter 4 - Synthesis gas production for FT synthesis, in Studies in Surface Science and Catalysis, A. Steynberg, Dry, M., Editor. 2004, Elsevier B.V. p. 697.
60. WBG, Nitrogenous Fertilizer Plants, in Pollution Prevention and Abatement Handbook. 1999, World Bank Group.
61. Marechal, F., Kalitventzeff, Boris, Computer-Aided Integration of Utility Systems, in Computer Aided Process and Product Engineering. 2006, Wiley-VCH Verlag GmbH. p. 327-381.
62. ASPENTECH, Aspen Plus V8.8, Aspen technology Inc. 2015: Bedford, United States.
63. Yoo, M., Lessard, L, Kermani, M., Maréchal, F. OSMOSE Lua: A Unified Approach to Energy Systems Integration with Life Cycle Assessment. in 12th International conference PSE 2015 and 25th International conference ESCAPE 2015. Copenhagen, Denmark.
64. Hotza, D., Diniz da Costa, J. C., Fuel cells development and hydrogen production from renewable resources in Brazil. International Journal of Hydrogen Energy, 2008. 33(19): p. 4915-4935.
65. Santos, V.E.N., Ely, R. N., Szklo, A. S., Magrini, A., Chemicals, electricity and fuels from biorefineries processing Brazil′s sugarcane bagasse: Production recipes and minimum selling prices. Renewable and Sustainable Energy Reviews, 2016. 53: p. 1443-1458.
66. Florez-Orrego, D., Sharma, S., Oliveira Jr, S., Marechal, F. Combined Exergy Analysis and Energy Integration for Design Optimization of Nitrogen Fertilizer Plants. in 30th International Conference on Efficiency, Cost, Optimization, Simulation and Environmental Impact of Energy Systems, ECOS, July 2 - 6, 2017. San Diego, US.
67. Nielsen, A., Ammonia: Catalysis and Manufacture. Vol. ISBN 9783540583356. 1995: Springer.
68. Florez-Orrego, D., Silva, J.A.M., Oliveira Jr, S., Renewable and Non-Renewable Exergy Cost and Specific CO2 Emission of Electricity Generation: The Brazilian Case. Energy Conv. and Management, v. 85, p. 619-629, 2014.
69. Flórez-Orrego, D., Silva, J.A.M., Velásquez, H., Oliveira Jr., S., Renewable and non-renewable exergy costs and CO2 emissions in the production of fuels for Brazilian transportation sector. Energy, v. 88, p. 18-36, 2015.

70. Florez-Orrego, D., Oliveira Junior, S. Comparative Exergy and Technoeconomic Assessment of Fossil and Biomass-Based Routes for Hydrogen and Ammonia Production. in International Conference on Contemporary Problems of Thermal Engineering - CPOTE, 2018. Gliwice, Poland.
71. Nakashima, R., Florez-Orrego, D., Oliveira Junior, S. Integration of Anaerobic Digestion and Biomass Gasification for combined Hydrogen, Biomethane and Power Production. in International Conference on Contemporary Problems of Thermal Engineering - CPOTE, 2018. Gliwice, Poland.
72. Strait, R., Nagvekar, M., Carbon dioxide capture and storage in the nitrogen and syngas industries. Nitrogen+Syngas. January-February 2010, (303).
73. CHEMCAD. Power Plant Carbon Capture with CHEMCAD. rev. 031109. Technical Articles. 2009 Accessed Oct. 12, 2014; Available at:
http://www.chemstations.com/content/documents/Technical_Articles/Power_Plant_Carbon_Capture_with_CHEMCAD.pdf
74. Seebregts, A.J., Gas-Fired Power. 2010, Energy Technology Systems Analysis Programme - IEA ETSAP - Technology Brief E02- April
75. Hamelinck, C., Faaij, A.P.C., Future prospects for production of methanol and hydrogen from biomass. Journal of Power Sources, 2002. 111(1): p. 1-22..
76. Mokhatab, S., Poe, W., Mak, J. Y., Chapter 6 - Natural Gas Treating, in Handbook of Natural Gas Transmission and Processing (Third Edition). 2015, Gulf Professional Publishing: Boston. p. 181-222.
77. Chen, C., A Technical and Economic Assessment of CO2 Capture Technology for IGCC Power Plants. 2005, Carnegie Mellon University: Pittsburgh, Pennsylvania.
78. Adams-Ii, T., Salkuyeh, Y., Nease, J., Chapter 6 - Processes and simulations for solvent-based CO2 capture and syngas cleanup A2 - Shi, Fan, in Reactor and Process Design in Sustainable Energy Technology. 2014, Elsevier. p. 163-231.
79. Florez-Orrego, D., Oliveira Jr, S., Modeling and optimization of an industrial ammonia synthesis unit: An exergy approach. Energy (Oxford), 2017. 137(15): p. 234-250.
80. Weston, C.W., Papcun, J. R., Dery, M., Ammonium Compounds, in Kirk-Othmer Encyclopedia of Chemical Technology. 2000, John Wiley & Sons, Inc.
81. Alves, L., Nebra, S. Exergoeconomic analysis in hydrogen production by Autothermal reforming of natural gas with Cogeneration. in 22nd International Conference on Efficiency, Cost, Optimization, Simulation and Environmental Impact of Energy Systems, August 31 – September 3. 2009. Foz do Iguaçu, Paraná, Brazil.
82.Gassner, M., Maréchal, F., Increasing Efficiency of Fuel Ethanol Production from Lignocellulosic Biomass by Process Integration. Energy & Fuels, 2013. 27(4): p. 2107-2115.